C.P. No. 958

C.P. No. 958

MINISTRY OF TECHNOLOGY

AERONAUTICAL RESEARCH COUNCIL

CURRENT PAPERS

Measurements of Drag, Base Pressure and Base Aerodynaniic Heat Transfer Appropriate to 8.5” Semi-Angle Sharp Cones in Free Flight at Mach Numbers from 0.8 to 3.8

by

G. H. Greenwood

LONDON: HER MAJESTY'S STATIONERY OFFICE

1967

TEN SHILLINGS NET

U.D.C. No. 533.696.24 : 533.6.048.2 : 533.6.011.6

C.P. 958*
December 1966

MEASUREMENTS OF DRAG, BASE PRESSURE AND BASE AERODYNAMIC HEAT TRANSFER APPROPRIATE TO 8·5° SEMI-ANGLE SHARP CONES IN FREE FLIGHT AT MACH NUMBERS FROM 0·8 to 3·8

by

G. H. Greenwood

SUMMARY

Measurements of drag, base pressure and aerodynamic heat transfer have been made on a sharp cone in free flight at Mach numbers up to 3·8 and free stream Reynolds numbers up to 77 millions based on cone length. The drag and base pressure measurements were in good agreement with estimates. The heat transfer data were however degraded by deficiencies in the construction of the thermocouples. Nevertheless they did show that the aerodynamic heat flux was uniform over the base. In particular there was no evidence of high values at the rear stagnation point.

---

*Replaces R.A.E. Technical Report 66394 - A.R.C. 29060.

CONTENTS

1 INTRODUCTION

This paper describes two separate experimental investigations with freely flying cones. The first of' these relates to heat transfer and surface pressures in regions of separated flow associated with backward-facing steps. Some results of this investigation relative to 15° semi-angle sharp cones having concentric sting attachments on the base are presented in Ref.1. In the present report similar data were obtained for a 8·5° semi-angle sharp cone flying freely without a sting attachment. The second investigation was concerned with the aerodynamic characteristics of freely flying cones. Such shapes are of interest in the context of satellite re-entry. Initially the investigations were limited to transonic and low supersonic speeds and to cones similar to those of the first investigation.

2 DESCRIPTION OF THE MODELS

Three models mere flown each consisting of a 8·5° semi-angle sharp cone having a base diameter of 10 inches. Two were designed to measure drag, base pressures and wall temperatures and are designated models 1 and 2. The remaining model, designated model 3, was designed to measure drag and base pressures only.

All the models were machined and polished to give centre-line average values of external surface finish of between 10 and. 20 micro-inches. Constructional details together with the location of pressure orifices are given in Fig. 1.

Models 1 and 2

The locations at which temperatures were measured are shown in Figs.1(a) and 2. These models mere designed to obtain heat transfer data appropriate to an area consisting of the base surface and the cone surface just ahead of the base. The latter surface is subsequently referred to as the cone skirt. The external walls of the cone skirt and base were made from mild steel, the mean thickness of the former being 0·040 inch and that of the latter 0·028 inch.

The models were fitted with polished metal reflectors located 0·1 inch from the internal surface of the calorimeter wall. These were intended to limit the radiation and convection of heat from the latter to the interior of the model. Another feature was a small gap of about 0.02 inch between the calorimeter wall of the base and the cone. This was incorporated to mitigate distortions arising from thermal expansions during flight and to eliminate effectively the conduction of heat from one component to the other.

Forward of the cone skirt the external wall of each model was made from steel in the form of a hollow cone which housed telemetry equipment and the ballast material necessary to adjust the weight and centre of gravity position.

<u>Model 3</u>

The construction of this model was similar to models 1 and 2 with the exception of the base region which, because temperature measurements were not required, consisted of a solid magnesium-alloy casting. Telemetry equipment was housed in the model forward of this component.

2.1 Telemetry aerials

The telemetry aerials on models 1 and 2 consisted of tuned semi-circular slots cut into the thin-walled base thus avoiding protruberances and hence flow disturbances ahead of the base (Fig.1(a)).

Two spike aerials were used on model 3. These protruded from the surface about 4 inches ahead of the base (Fig.1(b)). Model 3 was originally designed to measure longitudinal stability derivatives as well as drag and base pressures and in this original form had small lateral-thrust rocket motors attached to the base thus precluding *the* use of this area for accommodating the aerials.

2.2 Boosting arrangements

The boosting arrangements are illustrated in Figs.3 and 4. The models were mounted in tandem on their boost assemblies and were designed to separate from the latter under the influence of the drag and inertia forces after the rocket motors had ceased to thrust. In the case of the twin-boost arrangement for models 1 and 2 it was necessary to modify the boost nozzles. If nozzles aligned with the axes of the boost motors had been used on a twin-motor assembly a large thrust couple would have resulted if either of the motors had failed to ignite, thus constituting a potential range hazard. To minimise the couple arising in the event of such a failure and make the assembly safe to use on the Aberporth Range the thrust of each motor was directed through a point near the mean centre-of-gravity of the complete assembly by using nozzles at an angle to the axes of the motors.

3 INSTRUMSNTATION

All the models were equipped with inductance-type transducers to measure longitudinal and transverse accelerations and base pressures. Models 1 and 2 were additionally instrumented to measure wall temperatures using thermocouples attached to the internal surfaces of the calorimeter walls. Each thermocouple junction was constructed from 0.004 inch diameter chromel and alumel wires by arc welding the ends together to form a bead about 0.010 inch to 0.015 inch in diameter. This bead was then welded to the surface by means of a miniature spot welder. Recent laboratory measurements[3] however have shown that thermocouples formed in this way respond as if the junction were located some 0.010 inch from the surface.

A R.A.E. sub-miniature 465 M/cs telemeter was incorporated in all the models. In the case of models 1 and 2 it was modified to allow mixing of inductance and voltage types of input.

4 DESCRIPTION OF TESTS

Models 1 and 2 were launched at the R.A.E. Range at Aberporth. In each case the model and rocket-motor assembly was successfully tracked by the range instrumentation, namely kinetheodolites and reflection radio-Doppler up to the point of model separation. Thereafter the separated models were not tracked because of their small size and the remoteness of the ground tracking stations from the line-of-fire.

The telemetry records indicated that both these models were subjected to substantial impulsive forces at separation and in the case of model 1 all the thermocouples ceased to function subsequently. In the case of model 2 failure of fourteen thermocouples occurred out of a total of twenty-five - Fig.2 shows the location of those thermocouples from which usable data were obtained. The remaining instruments in these models functioned satisfactorily throughout the flight.

Model 3 was launched at the R.A.E. range at Larkhill and was successfully tracked by kinetheodolites throughout flight.

Trajectory data appropriate to each model are presented in Figs.5-7. Atmospheric pressure, density and temperature relevant to the flight altitudes were obtained by the usual range procedures[2].

5 DATA REDUCTION

5.1 Trajectory

Where possible, velocity and space co-ordinates were derived from data given by the range instruments external to the models, that is by kinetheodolites and reflection Doppler. Such data, however, were not available for models 1 and 2 after separation from their booster assemblies. and a different procedure referred to subsequently as method A had to be adopted. In these cases velocity and space co-ordinates were integrated from the telemetered measurements of deceleration assuming a ballistic flight path.*

The initial conditions for this integration process were those appropriate to the complete assembly at the instant of model separation.

The velocities determined in this way were sensitive to uncertainties in the initial conditions because the actual instant of model separation is difficult to establisn. They were also sensitive to uncertainties in the telemetered measurements of deceleration. Thus the reliability of the velocity data for models 1 and 2 was not so good as that for model 3 where kinetheodolite coverage was obtained throughout the flight.

For the reasons noted in section 6.1 the trajectory data for model 2 after separation wore also determined independently of either the model-borne or range instrumentation. In this procedure, referred to subsequently as method B, it was assumed that the flight path was ballistic and that the variation of drag coefficient with Mach number was the same as that determined for model 1.

5.2 <u>Drag and base pressure measurements</u>

Drag and base-pressure coefficients were derived using the telemetered longitudinal-accelerometer and base-pressure data respectively. The reduction procedures used are as described in Ref.2.

5.3 <u>Temperature measurements</u>

From the measurements of wall temperature values of heat flux to each station were obtained. These values represent nett quantities, q_{nett}, where:-

$$q_{nett} \doteq q_{aero} + q_{lateral} - q_{radiation} - q_{air\ conduction} - q_{free\ convection} \quad (1)$$

These terms are defined in the list of symbols.

The data reduction procedure used assumes that the thermocouples sense directly the temperature of the internal surface of the walls. Ref.3 shows that this assumption is not accurate for the bead-type thermocouple construction used in the present tests. Unfortunately, however, adjustments

---

*The assumption of a ballistic flight path was substantiated by the response of the transverse accelerometers which showed these models were subjected to negligible side forces.

for this effect arc not practical except during the initial stages of flight and have not been attempted in the present instance.

Because of the uncertainties in the measurement of the heat flux near zero-heat-transfer conditions and because of the lack of precise information regarding the magnitude of the non-aerodynamic heat fluxes no reliable determination of recovery factors could be made. The heat-transfer data were therefore reduced assuming a constant value of recovery factor of 0·89 relative to free-stream conditions; this assumed value was based on the wind-tunnel data summarised in Ref.&

5.3.1 Reference heat fluxes

The experimental aerodynamic heat flux at each station, q_m, was compared with two theoretical heat fluxes:

(a) q_{fp}, the flat plate value of aerodynamic heat flux appropriate to free-stream conditions, a turbulent boundary layer and local wall temperature evaluated in accordance with Eckert's intermediate enthalpy theory as described in Ref.5. The relevant length of boundary-layer run was taken as half the wetted length from the apex to the station in the case of stations on the cone skirt and as half the wetted length from the apex to the base in the case of stations *on* the base. Since no account is taken of variations in local conditions in the determination of q_{fp} it is not a likely medium for collapsing data completely. It does however permit some appreciation of relative magnitudes in that it can be used to normalise data with respect to wall temperature and reference length.

(b) q_ℓ, evaluated in the same way as q_{fp}, except that instead of taking conditions outside the boundary layer *to* correspond to the free *stream* they were considered to be appropriate to the estimated local-flow conditions just outside the boundary layer for stations on the cone and just outside the initial wake boundary for stations on the base. Theoretically the ratio q_m/q_ℓ should be unity for stations on a cone of uniform temperature with a boundary layer turbulent from the apex. Thus the ratio may be regarded as a convenient measure of the applicability of the theory of Ref.5 for predicting the heat flux to the cone skirt and of taking some account of variations in local conditions in the case of stations on the base.

In the case of stations on the cone skirt a third reference heat flux was used. This heat flux, $q_{\ell n}$, was estimated on a similar basis to q_ℓ above, but with some account taken of non-isothermal effects. The calculations of

$q_{\ell n}$ were based on the theory of Ref.6. It was assumed that the temperature of the forebody ahead of the cone shirt remained at its initial temperature at launch throughout flight, that is at the measured atmospheric temperature at ground level, namely 284°K.

6 RESULTS AND DISCUSSION

6.1 Drag and base pressures

The variation of drag and base pressure with Mach number for the models is presented in Figs.%-12. The measurements of drag for models 1 and 3 are given in Figs.8(a) and (b) respectively. The total drag relationships for all the models are compared in Fig.9. The data for the base pressure are presented in a similar manner in Figs.10(a) to 10(c) respectively and compared in Fig.11.

Fig.8 include estimates [7] of turbulent skin-friction drag assuming that the surface temperature remains at the ambient temperature at launch throughout flight. An estimate of the isolated drag of the aerials on model 3 based on Refa.7 and 8 is included also in Fig.8(b).

In Fig.8 the trajectory data for models 1 and 2 were obtained by integrating telemetered accelerometer records (method A of section 5.1) and that for model 3 from kinetheodolite data. In order that the total-drag data for the cones should be directly comparable the estimated isolated drag of the aerials has been subtracted from the total drag of model 3.

It is apparent from Fig.9 that at supersonic speeds the drags of models 1 and 3 are in fair agreement and that of model 2 is discrepant from both. At high subsonic speeds differences between the determinations of drag for the models are more likely to be greater than at supersonic speeds, through the rapid changes in drag that occur then and consequent limitations in the accuracy of the reduction procedures. More weight is therefore accorded to the drag measurements at supersonic speeds and here one would expect little variation between models since the shapes, surface finish and test environment were similar, particularly in the case of models 1 and 2. Therefore it is presumed that the accelerometers from which the trajectory data for model 2 were derived had not functioned accurately. Trajectory data as derived by method B (section 5.1) are used elsewhere - that is, it was assumed that the total drag relationship for model 1 in Fig.8 also obtained for model 2.

The differences between the Mach number histories for model 2 derived by methods A and B are shown in Fig.6. They mere less than 0·08 in Mach number above Mach 1. These differences are equivalent approximately to a three per cent difference in acceleration - that is an amount somewhat higher but nevertheless comparable with the accuracy of the telemetry equipment.

The detailed plots of base pressure for each orifice position shown in Fig.10 indicate that no significant pressure gradients existed over the base. Therefore base drag coefficients were derived assuming mean values of the measured pressure to exist over the entire base area. The departure from a smooth variation with Mach number of the pressure from orifice PI on model 1 apparent in Fig.10(a) is implausible. The results from orifices in a similar position on the other models do not show this feature and the possibility of a spurious response from tho pressure transducer cannot be discounted.

In Fig.11 a comparison is made between the base pressures for the three models. At supersonic speeds the measurements are consistently within the expected uncertainties. At subsonic speeds the measurements are less consistent and it is possible that the differences may be due in part to the increasing uncertainty in assessing trajectory data for models 1 and 2 as flight time increases. In the case of model 3 some of the difference may be due to interference effects arising from the protruding aerials. For example in Ref.9 the presence of protruberances in the form of fins ahead of a base has been shown to result in increased base pressures, the greatest increase occurring at subsonic speeds.

Sharp peaks occur in the base pressure coefficients of all models near sonic speeds. This is qualitatively consistent with the data summarised by Nash in Ref.10 where similar trends on the blunt trailing-edges of aerofoils are noted. The maxima measured in the present test are seen to vary between models both in magnitude and in the Mach number at which they occur but these variations may be due in part at least to experimental uncertainty.

Base pressure coefficients appropriate to a 9° semi-angle cone having a cylindrical sting attached to the base are also included in Fig.11 for Mach numbers from 3·5 to 9·0. These coefficients are from Ref.15 and acre obtained at Reynolds numbers substantially lower than those for the present tests.

The base pressure measurements at supersonic speeds for all the models are compared in Fig.10 with estimates based on the method proposed by Chapman in Ref.11. The basis of this method is the use, in conjunction with an empirical correlation curve, of the static pressure and Mach number estimated at some point on a hypothetical streamwise extension of the cone base. The precise location of the point at which these quantities are estimated is conjectural. It would appear to depend largely on the extent of the dead-air region in the base wake.. Chapman proposes that a point at one base diameter downstream of the real base be used.. In Ref. 12, however, Whitfield and Potter obtained a better prediction of the base pressure measurements mode on a 9° semi-angle sharp cone. They used values of static pressure and Mach number estimated at a point immediately downstream of the real base together with a modified form of Chapman's empirical correlation.

The estimates of base pressure in Pig.10 were made for the present model configuration using the methods of Refs. 11 and 12 without change. It can be seen that the present data lie generally between the estimates from both sources.

In Pig.12 theoretical[13] values of the cone wave drag are compared with those derived from models 1 and 3. Tho experimental data represent the residual drag after the measured base drag, estimated[7] skin-friction'drag and, in the case of model 3 the estimated[7,8] aerial drag have been subtracted from the total drag measured for each model. There is good agreement between the estimated and experimental values of wave drag. The discrepancy is everywhere less than five por cent of the total drag coefficient. Some of this dis-orepancy might be attributed to uncertainties in the estimates of the skin friction and aerial drag.

6.2 Heat transfer

Heat transfer data were obtained only from model 2. Although model 1 was also instrumented to measure heat transfer no information was obtained from it due to a fault in the telemetry equipment arising probably from the dis-turbance at model separation. The results from model 2 wore from eight stations on the base and three stations on the cone skirt in the positions shown in Fig.2. No results were obtainod from the remaining stations possibly due to a breakage of the thermocouples during the separation disturbance.

Fig.13 shows the variation with flight time of the mean temperature measured on the cone skirt and base together nith upper and lower limits representing the maximum and minimum temperatures at individual stations. Apart from station S12 on the. cone skirt it is seen from Fig.13 that the maxi-mum variation between stations is everywhere less than 30K° on the base and 15K° on the cone skirt.

Estimated values of the principal non-ncrodynsmic heat fluxes in equa-tion (I) are presented for typical stations on the cone skirt and base in

Fig.14 assuming the values for the wall emiaaivitiea and temperature of the radiation shield are as specified in Table 1. The maximum total non-aerodynamic heat flux is about 0·75 CHU ft^{-2} aec^{-1} on the cone skirt and 0·15 CHU ft^{-2} sec^{-1} on the base. Since for the moat part these quantities are small compared to the nett heat flux except of ccurae near zero heat transfer conditions and ore also subject to some computing uncertainty it has been assumed that the aerodynamic heat flux is equal to the nett heat flux for all stations except S12. The lower temperature at station S12 during decelerating flight is qualitatively consistent with the proximity (0·25 inch) of this station to the cooler bulk of the cone forebody (see Fig.2). Typical distributions of' temperature and aerodynamic heat flux to the cone skirt and base at several Mach numbers are presented in Fig.15. The variation of these quantities with Mach number for the stations on the cone skirt end the base are presented in Fig.16.

6.2.1 Heat transfer to cone skirt

During accelerating flight, when the model was mounted on the boost assembly, the temperatures measured at the three stations on the cone skirt were approximately equal at constant Mach number and the nett heat flux was approximately uniform along the surface.

During decelerating flight, after the model had. separated from the boost assembly, the temperature measured at station S12 indicated a considerable gradient along the cone skirt. This was attributed to the proximity of S12 to the heat sink formed by the bulk of the model (Fig.2) and the heat flux to this station was corrected for an estimated lateral heat flux on the assumption that the heat sink remained at the launching temperature of 284°K throughout flight. With this correction the variation of the aerodynamic heat transfer coefficients at station S12 were similar to those obtained at the other stations on the cone skirt.

6.2.2 Comparison with reference heat fluxes

In Fig.16 the theoretical heat fluxes q_{ℓ} and $q_{\ell n}$ are compared with the experimental heat flux to the cone skirt. The theoretical values are those appropriate to a flat plate in the local flow conditions existing just outside a turbulent boundary layer over the cone. At all stations on the cone skirt during accelerating flight the experimental values are in better agreement with the theoretical values relevant to an isothermal surface, q_{ℓ}.

During decelerating flight the measurements are in better agreement with the non-isothermal values of the theoretical heat flux, $q_{\ell n}$, particularly as maximum temperature on the cone skirt is approached at approximately $M = 3$.

Although there is apparently close agreement between the experimental and theoretical heat fluxes to the cone skirt during accelerating flight this result was obtained us-ing a thermocouple construction which is now believed [3] to give rise to determinations of heat flux somewhat lower than the true magnitude. Since no correction to take account of thermocouple construction has been attempted such close agreement between experiment and theory is unexpected. It may be that the thermocouple construction effect has been oancelled by some other unidentified factor. For example, the effects of interference between the boost assembly and cone skirt could result in heat fluxes greater than those predicted by theory which assumes flow conditions free from interference on the cone skirt.

6.2.3 Heat transfer to base

No heat transfer data during accelerating flight were obtained for the base surface because it was shrouded by the boost assembly for that part of the flight. During decelerating flight the variations in temperature and heat flux at a given Mach number at the various stations illustrated in Fig.15 are comparable to the accuracy of the measuring technique and therefore cannot be interpreted as significant.

The experimental heat fluxes to the cone base are compared with the reference heat fluxes q_ℓ and q_{fp} in Fig.17. This comparison is presented in the form of ratios q_m/q_ℓ and q_m/q_{fp} against Mach number, where q_m is the experimental heat flux and q_ℓ and q_{fp} are as defined in section 5.3.1. The curves of Fig.17 have been drawn through a considerable scatter in the measurements from the individual measuring stations. The extent of this scatter is indicated in the figure.

Near zero heat transfer conditions between $M = 1{\cdot}6$ and 2.5, the magnitude of the measured heat flux was comparable to the experimental uncertainties and the scatter in the ratios, q_m/q_ℓ and q_m/q_{fp}, was such that no data for this region have been presented.

Fig.17 indicates that the mean heat flux to the cone base at speeds above $M = 2{\cdot}5$ was about 0·15 times the theoretical reference heat flux to a flat plate at zero incidence in the free stream, q_{fp}, and about 0·3, rising to about 0-7 at $M = 3{\cdot}81$, times the theoretical reference heat flux to the wake boundary assuming the latter to be replaced by a solid surface, q_ℓ. At speeds below $M = 1 \cdot 6$ the scatter in the ratios is generally larger than at the higher Mach numbers and the relevant data must be regarded as being less reliable. Both the ratios, however, show a trend towards unity with decreasing Mach number.

6.2.4 Comparison with other tests

In Fig.18 the mean heat flux to the cone base at $M = 3 \cdot 5$ from the present tests is compared with similar measurements reported in Ref.1. The latter measurements were made using 15° semi-angle cones (compared with 8·5° for the cones in the present test) having a step down to a cylindrical sting attached to the base. The ratio of sting diameter to base diameter was varied between these models. Measurements were made of the heat flux to the model surface in the separated flow region aft of the step.

In Fig.18 the ratio, q_m/q_ℓ, is plotted against the ratio of sting diameter to base diameter for the two models from Ref.1 (where the flow reattached on the sting) and for the present tests. The latter corresponds to the case of zero, sting diameter. Fig.18 suggests that q_m/q_ℓ is not strongly dependent on the ratio of sting diameter to base diameter. That q_m/q_ℓ over the cone base without a sting is apparently greater than for cones with stings does not necessarily signify a trend. It may be attributable in part to experimental uncertainty and in part to the differences in cone angle between the models of Ref.1 and those of the present tests.

A particular feature of the present results is the approximate uniformity in heat flux over the cone base at constant Mach number. It is of interest to note that in the test of Ref.14 substantial variations were found in the heat transfer rates over the blunt base of a hemisphere-cylinder at constant Mach number with the highest heating rate occurring at the base centre. These latter results, obtained in a shock tube at shock Mach numbers between 3·5 and 4·0, refer to a forebody shape different from that used in the present tests and to flow conditions where the establishment of a steady equilibrium wake flow was probably not achieved.

7 CONCLUSIONS

Measurements of total drag, base pressure and aerodynamic heat flux have been made on a 8·5° semi-angle, sharp cone in free flight over a Mach number range of 0·8 to 3·8 and at free-stream Reynolds numbers between 5 and 26 millions per foot. The measured pressures and aerodynamic heat fluxes mere approximately uniform over the cone base at constant Mach number.

The measured base pressures at supersonic speeds are in fair agreement with estimates based on Chapman's method[11].

The measurements of total drag and base pressure were used in conjunction with estimates of skin friction drag to derive the cone wave drag. The wave drag was in good agreohent with Kopal's theory.

The magnitude of the mean heat flux to the cone base at Mach numbers above 2·5 was approximately 0·15 times that appropriate to a flat plate at zero incidence in the free stream and approximately 0·3, rising to 0·7, times that appropriate to a solid surface replacing the wake boundary.

The measured heat fluxes to the cone skirt during the heating phase of the flight were in good agreement with theoretical values based on flat plate theory, these measurements mere, however, subject to some uncertainty arising from deficiencies in the thermocouple construction used and from possible interference effects between the boost motor assembly and model.

A limited comparison between the present tests at $M = 3{\cdot}5$ and those of Ref.1 indicate that the magnitude of the heat flux to the base of the cone at zero incidence and free from base attachments is not markedly different from that to cones having concentric cylindrical sting attachments on the base.

Table 1

Data for estimating non-aerodynamic heat fluxes

Thermocouple stations		Cone skirt	Base	units
Emissivity factor of measuring wall	External surface, ε_e	0.76	0·20	-
	Internal surface, ε_i	0·76	0·20	-
Emissivity of radiation shield, ε_s		0·08	0.08	-
Temperature of radiation shield, T_s		300	300	^oK

SYMBOLS

C_D	drag coefficient $= (\text{drag})/q_o S$	
$C_{D\,aerials}$	aerial drag coefficient for model 3 $= (\text{aerial drag})/q_o S$	
$C_{D\,base}$	base drag coefficient $= (\text{base drag})/q_o S$	
$C_{D\,skin}$	skin friction coefficient $= (\text{skin friction drag})/q_o S$	
C_{D_W}	wave drag coefficient $= (\text{wave drag})/q_o S$	
C_{p_b}	base pressure coefficient $= (p_b - p_o)/q_o$	
k_a	mean thermal. conductivity of air in the temperature range between T_S and T_W	CHU ft^{-1} $(°C)^{-1}$ sec^{-1}
M	free-stream Mach number	
p_b	measured base pressure	lb/ft^2
p_o	free-stream static pressure	lb/ft^2
q_{aero}	aerodynamic heat flux	CHU ft^{-2} sec^{-1}
q_{air} conduction	heat flux conducted across internal air gap $\doteqdot k_a(T_W - T_S)/\tau_a$	CHU ft^{-2} sec^{-1}
$q_{external}$ radiation	local heat flux arising from radiation from external surface of the measuring wall $= \beta\, \varepsilon_e\, T_W^4$	CHU ft^{-2} sec^{-1}
q_{fp}	theoretical aerodynamic heat flux appropriate to free-stream conditions	CHU ft^{-2} sec^{-1}
q_{free} convection	additional heat flux across air gap' arising from free convection	CHU ft^{-2} sec^{-1}
q_ℓ	theoretical aerodynamic heat flux appropriate to local conditions	CHU ft^{-2} sec^{-1}
$q_{lateral}$	change in nett local heat flux arising from temperature gradients along the measuring wall	CHU ft^{-2} sec^{-1}
$q_{\ell n}$	theoretical aerodynamic heat flux q_ℓ adjusted to non-isothermal wall conditions	CHU ft^{-2} sec^{-1}
q_m	experimental aerodynamic heat flux	CHU ft^{-2} sec^{-1}
q_{nett}	nett local heat flux	CHU ft^{-2} sec^{-1}

SYMBOLS (Contd.)

$q_{\text{nett internal radiation}}$	nett local heat flux arising from radiation from the internal surface of the measuring wall $= \beta\,[1/\varepsilon_i + 1/\varepsilon_s - 1]^{-1}\,[T_W^4 - T_S^4]$	CHU ft^{-2} sec^{-1}
$q_{\text{radiation}}$	nett local heat flux arising from radiation from both surfaces of the measuring wall	CHU ft^{-2} sec^{-1}
q_o	free-stream dynamic pressure	lb/ft^2
S	reference area = base area of cone (= 0·545 ft^2)	ft^2
T_S	temperature of radiation shield	°K
T_W	temperature of measuring wall	°K
β	Boltzmann's constant $= 2.78 \times 10^{-12}$ CHU ft^{-2} sec^{-1} (°K)^4	
ε_e	emissivity factor of measuring wall external surface	
ε_i	emissivity factor of measuring wall internal surface	
ε_s	emissivity factor of radiation shield surface	
τ_a	thickness of air gap between internal surface of measuring wall and radiation shield (= 0·0083 ft)	ft

REFERENCES

No.	Author	Title, etc.
1	J. Pioken	Free-flight measurements of pressure and heat transfer in regions of separated and reattached flow at Mach numbers up to 4.0. A.R.C. C.P. 706, September 1960
2	J. A. Hamilton P. A. Hufton	Free flight techniques fcr high speed aercdynamic research. Jour. R. Ae. Soc., pp. 151-177, March 1956
3	F. H. Irvine J. Picken G. H. Greenwood	Measurements of the response of various thermocouple arrangements. R.A.E. Technical Note No. Aero 2959, (A.R.C. 26187) April 1964
4	R. J. Monaghan	Formulae and approximations for aerodynamic heating rates in high speed flight. A.R.C. C.P. 360, October 1955
5	L. F. Crabtree R. L. Dommett J. G. Woodley	Estimation of heat transfer to flat plates, cones and blunt bodies. R.A.E. Technical Report No. 65137, (A.R.C. 27233) July 1965
6	J. P. Hartnett E. R. G. Eckert R. Birkebek	Calculation of convective heat transfer to non-isothermal surfaces exposed to a fluid. stream with wedge type surface pressure gradient. W.A.D.C. Technical Report No. 57-733, D.109964, July 19%
7		Handbook cf supersonic aerodynamic data. Vcl. 2, Chapter 5.5, R.A.E. GW/Handbook/1
8	C. J. Welsh	The drag of finite-length cylinders determined from flight tests at high Reynolds numbers for a Mach number range from 0.5 to 1.3. N.A.C.A. T.N. 2941, June 1953
9	R. G. Hart	Effects of stabilising fins and a rear-support sting on the base pressures of a body of revolution in free flight at Mach numbers from 0.7 to 1.3. N.A.C.A. RM. L52E06, September 1952

REFERENCES (Contd.)

No.	Author	Title, etc.
10	J. F. Nash	A review of research on two-dimensional base flow. N.P.L. Aero Rept. 1006, March 1962
11	D. R. Chapman	An analysis of base pressure at supersonic velocities and comparison with experiment. N.A.C.A. Rept. 1051, 1951
12	J. D. Whitfield J. L. Potter	On base pressures at high Reynolds numbers and hypersonic Mach numbers. AEDC-TN-60-61, March 1960
13	Z. Kopal	Tables of supersonic flow around cones. M.I.T. Dept. of Elec. Eng. Center of Analysis Technical Report 1, 1947
14	J. Rabinowicz	Measurements of turbulent heat transfer rates on the aft portion and blunt base of a hemisphere-cylinder in the shock tube. Guggenheim Aeronautical Laboratory, Calif. Institute of Technology, Research Project Memorandum No. 41, November 1957
15	N. A. Zarin	Base pressure measurements on sharp and blunt 9° cones at Mach numbers from 3.5 to 9.2. Unpublished American Report

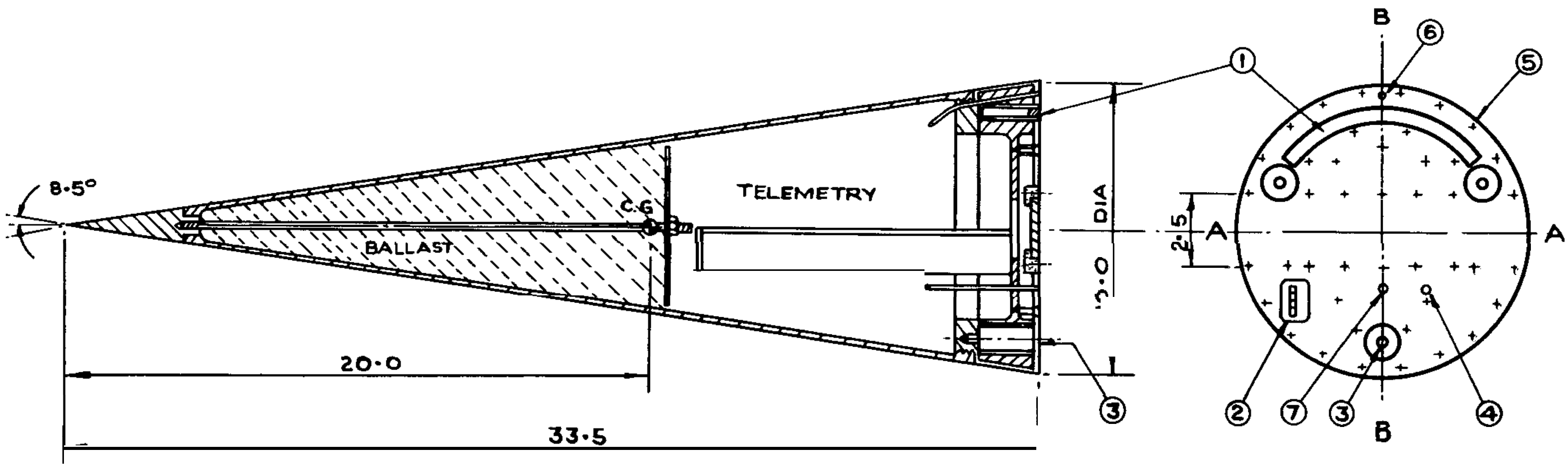

① TELEMETRY AERIAL
② EXTERNAL POWER SUPPLY SOCKET
③ LAUNCHING - SPIGOT LOCATIONS
④ SLAVE AERIAL CONNECTION
⑤ COUNTER-SUNK FIXING SCREWS
⑥ PRESSURE ORIFICE p1 (4·5 in FROM CENTRE)
⑦ PRESSURE ORIFICE P2 (2·0 in FROM CENTRE)

THERMOCOUPLES ARE IN PLANE A - A

(DIMENSIONS IN INCHES)

SECTION ON B-B

FIG. 1a GENERAL ARRANGEMENT OF MODELS 1 & 2

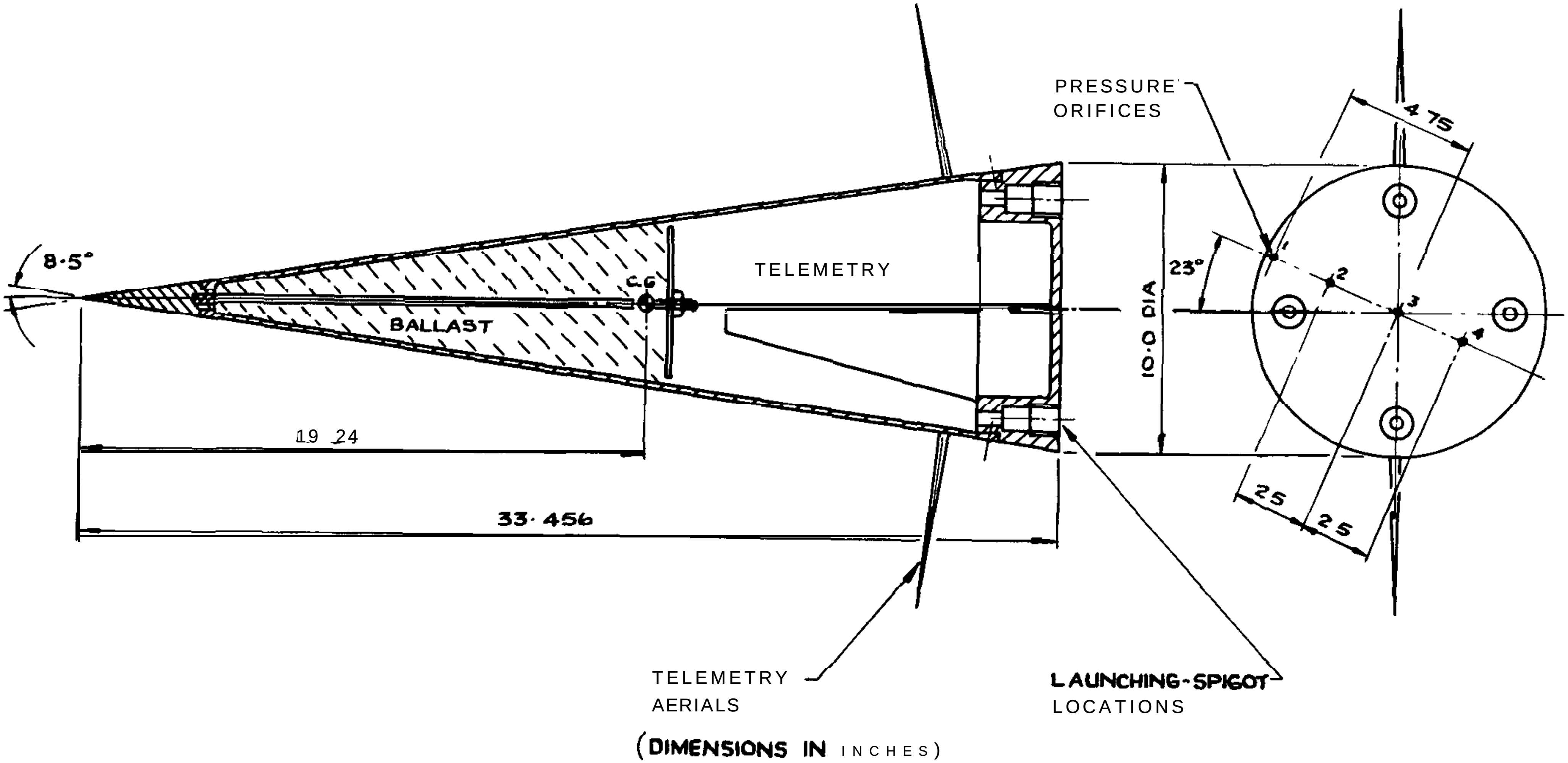

FIG. lb GENERAL ARRANGEMENT OF MODEL 3

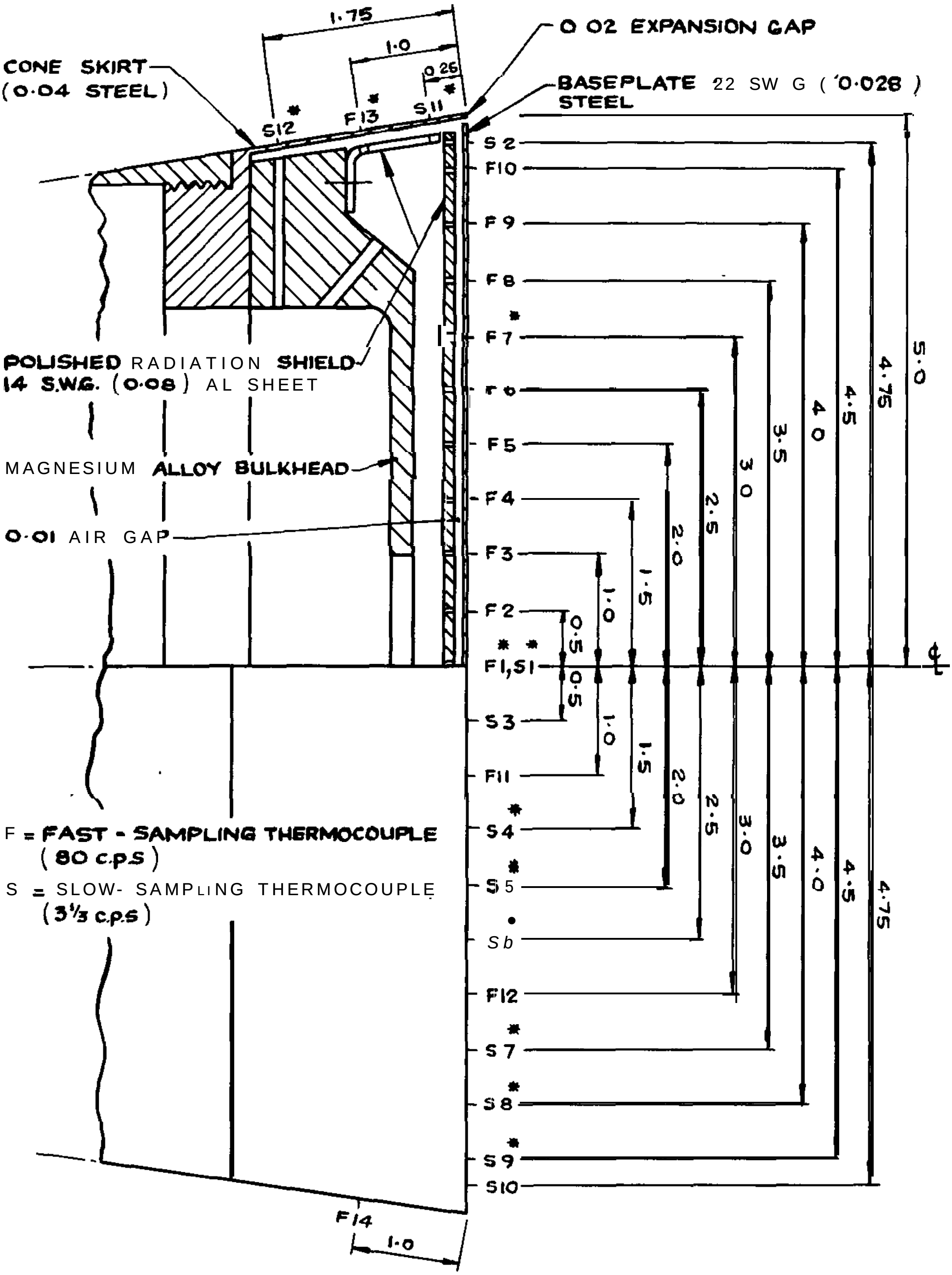

* THERMOCOUPLES FROM WHICH RESULTS WERE OBTAINED (MODEL 2)

(DIMENSIONS IN INCHES)

HALF SECTION ON A-A (FIG la)

FIG 2 LOCATION OF THERMOCOUPLE STATIONS ON MODELS I AND 2

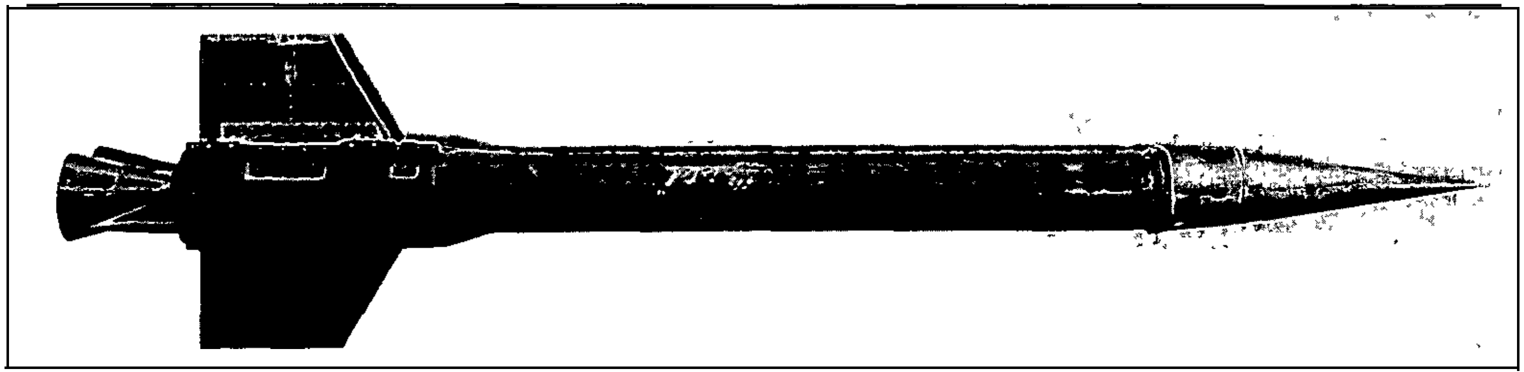

Models 1 & 2

Model 3

Fig.3. Test vehicles

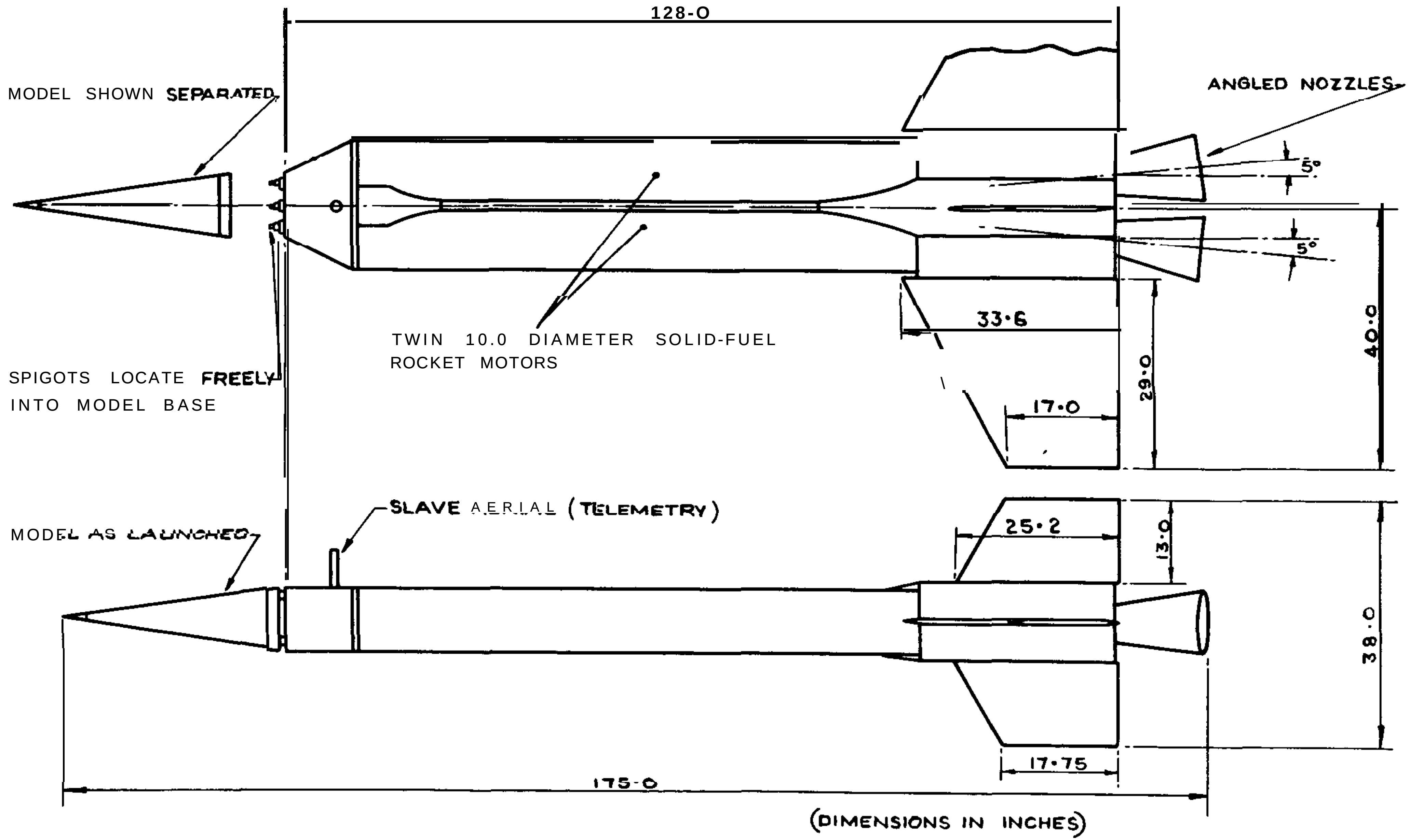

FIG. 4a DETAILS OF BOOSTING ARRANGEMENT — MODELS 1 AND 2

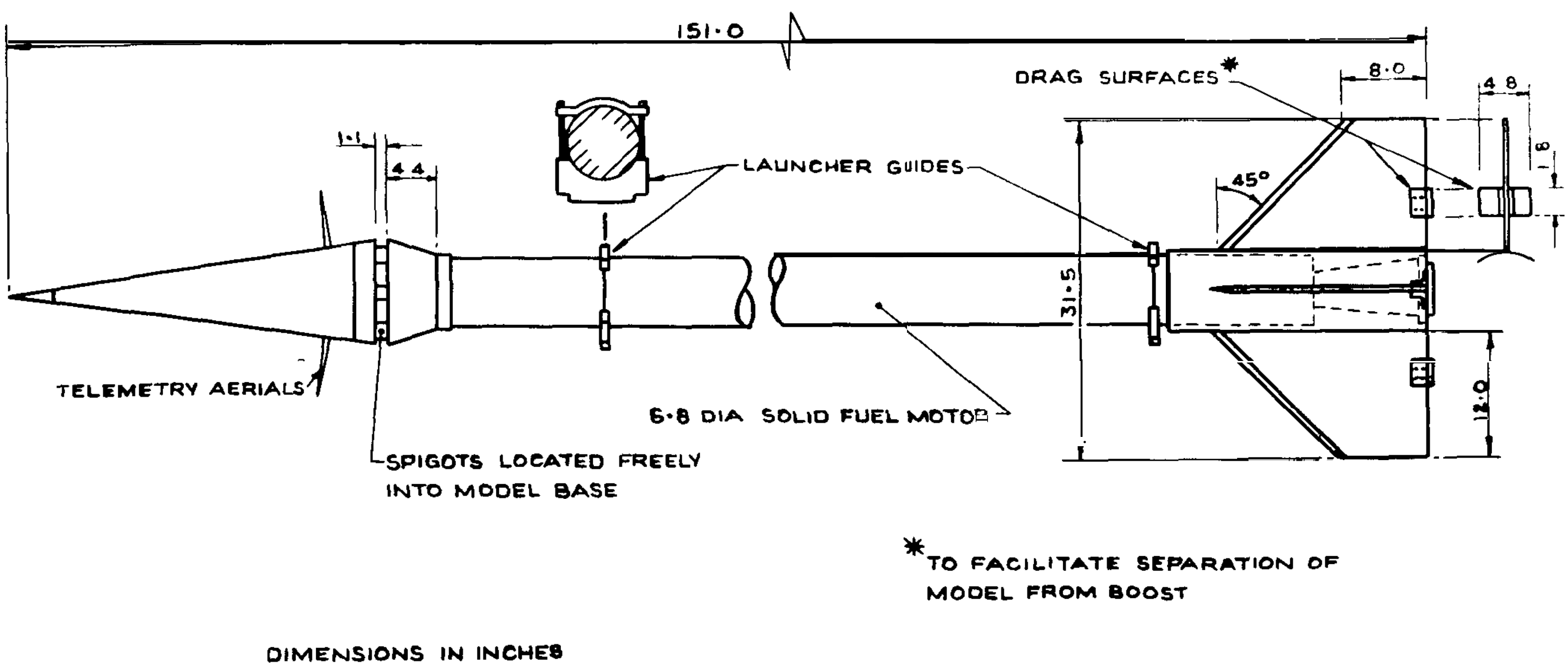

FIG. 4b DETAILS OF BOOSTING ARRANGEMENT – MODEL 3

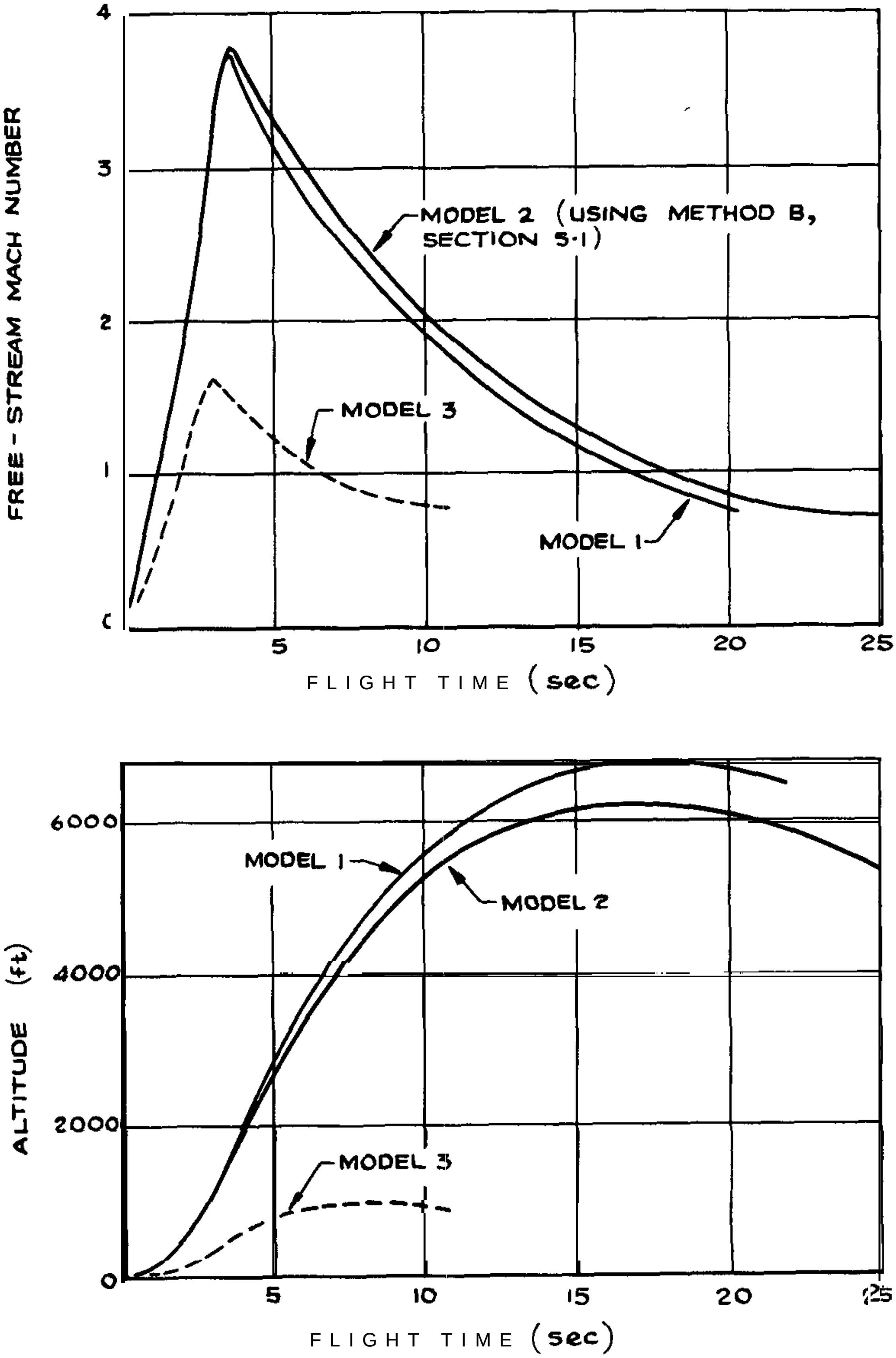

FIG. 5 TRAJECTORY DATA

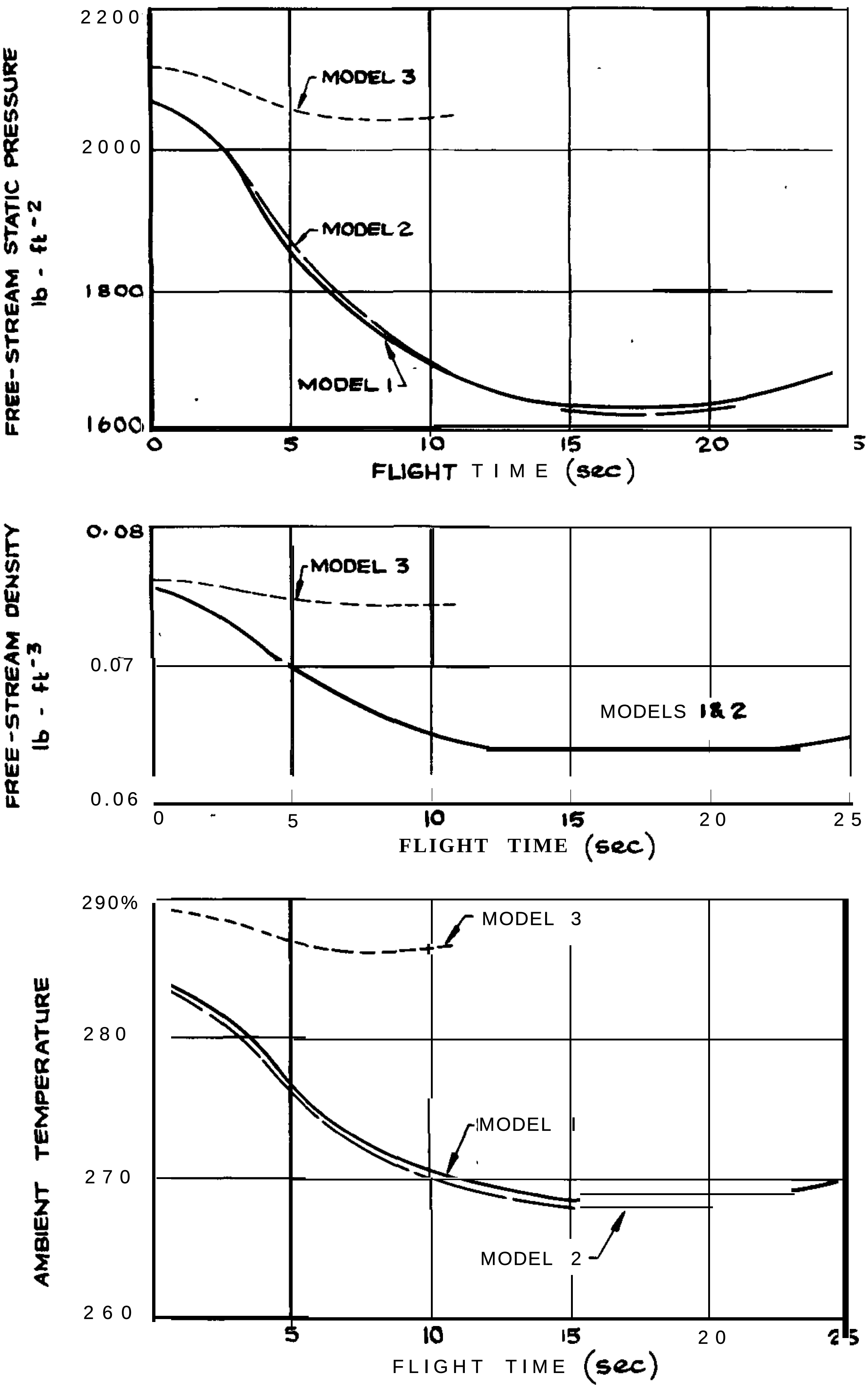

FIG 5 contd TRAJECTORY DATA

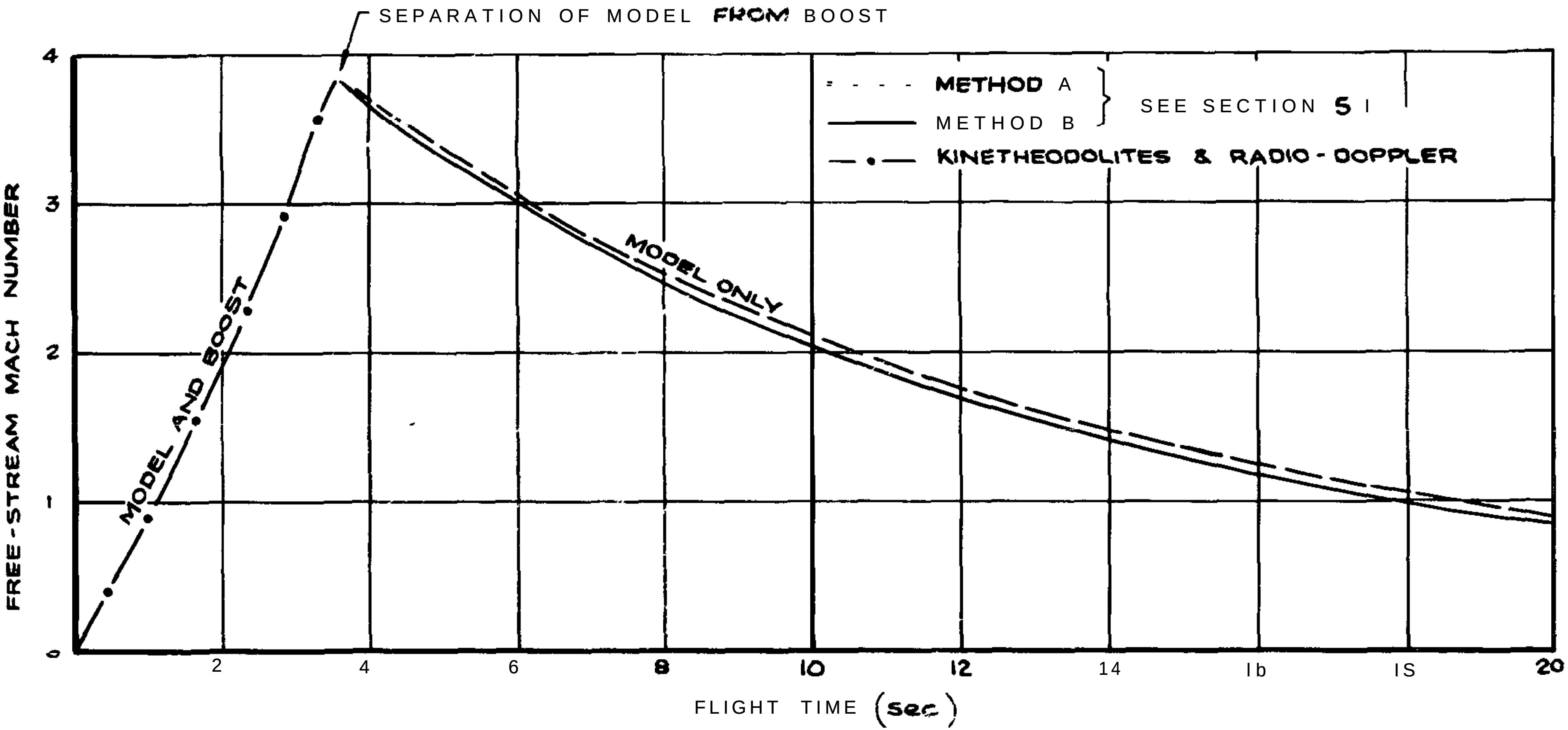

FIG. 6 COMPARISON OF MACH NUMBER DETERMINATIONS FOR MODEL 2

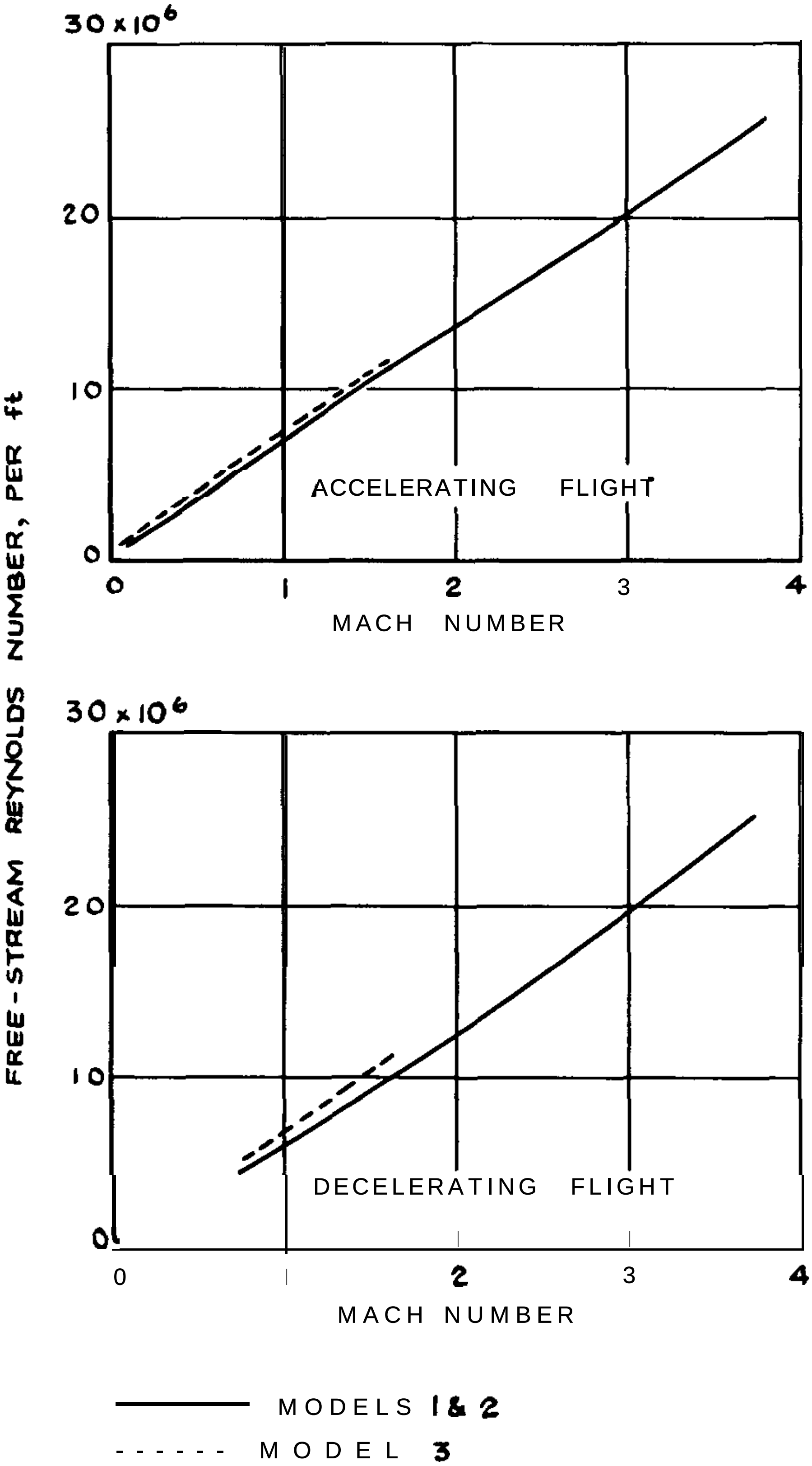

FIG. 7 VARIATION OF FREE- STREAM REYNOLDS NUMBER WITH MACH NUMBER

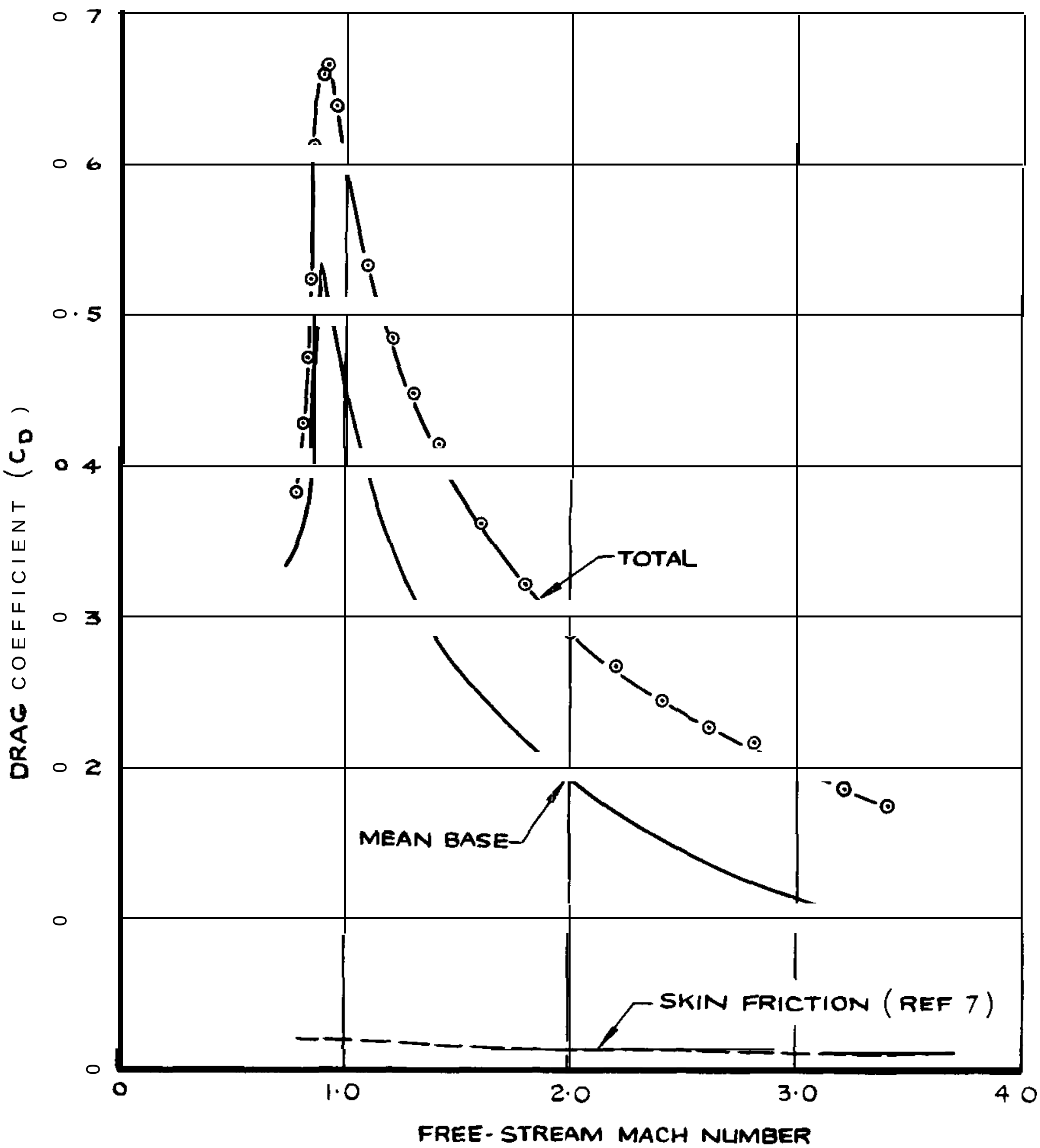

FIG. 8a VARIATION OF DRAG WITH MACH NUMBER FOR MODEL I

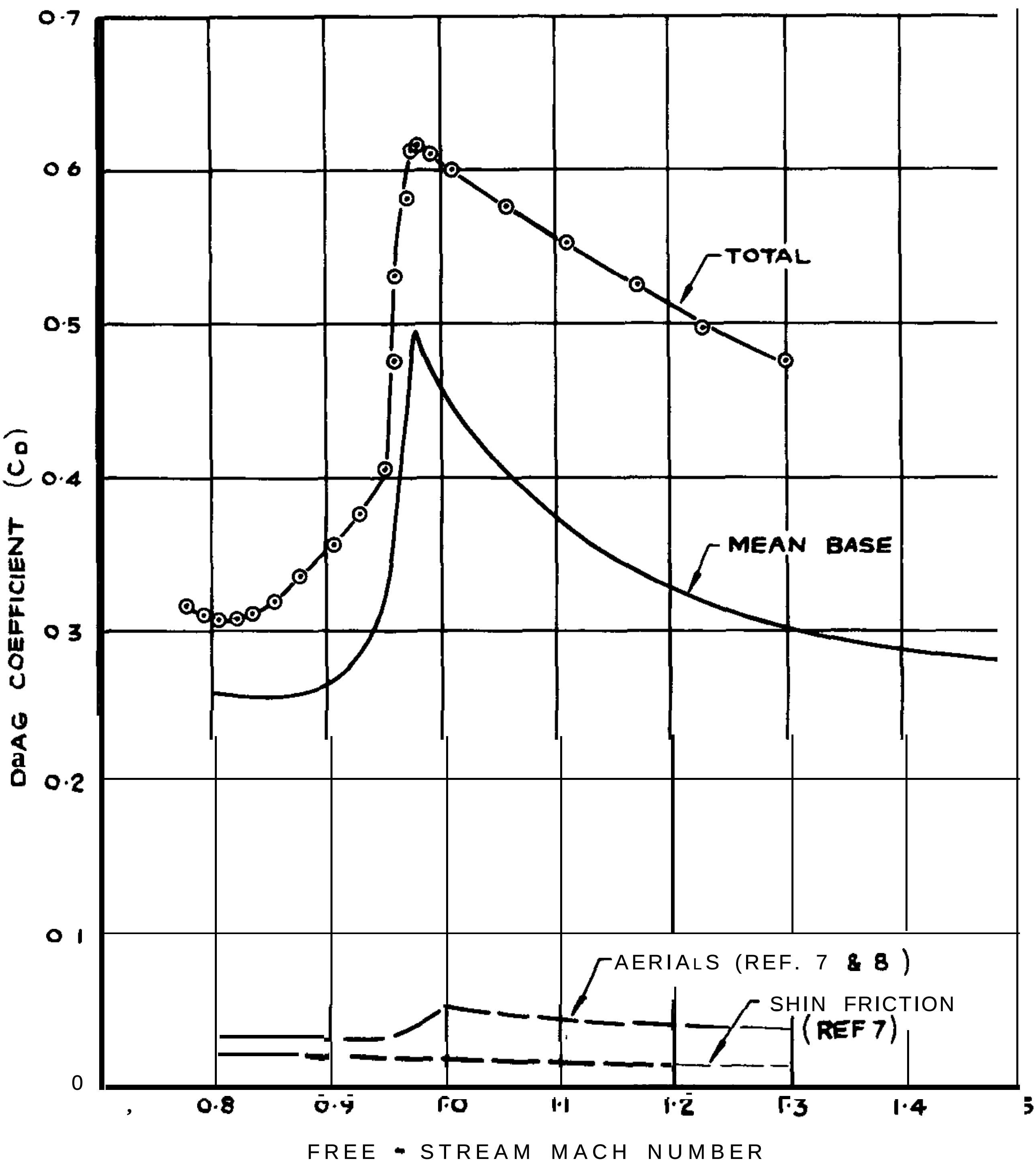

FIG. 8b VARIATION OF DRAG WITH MACH NUMBER FOR MODEL 3

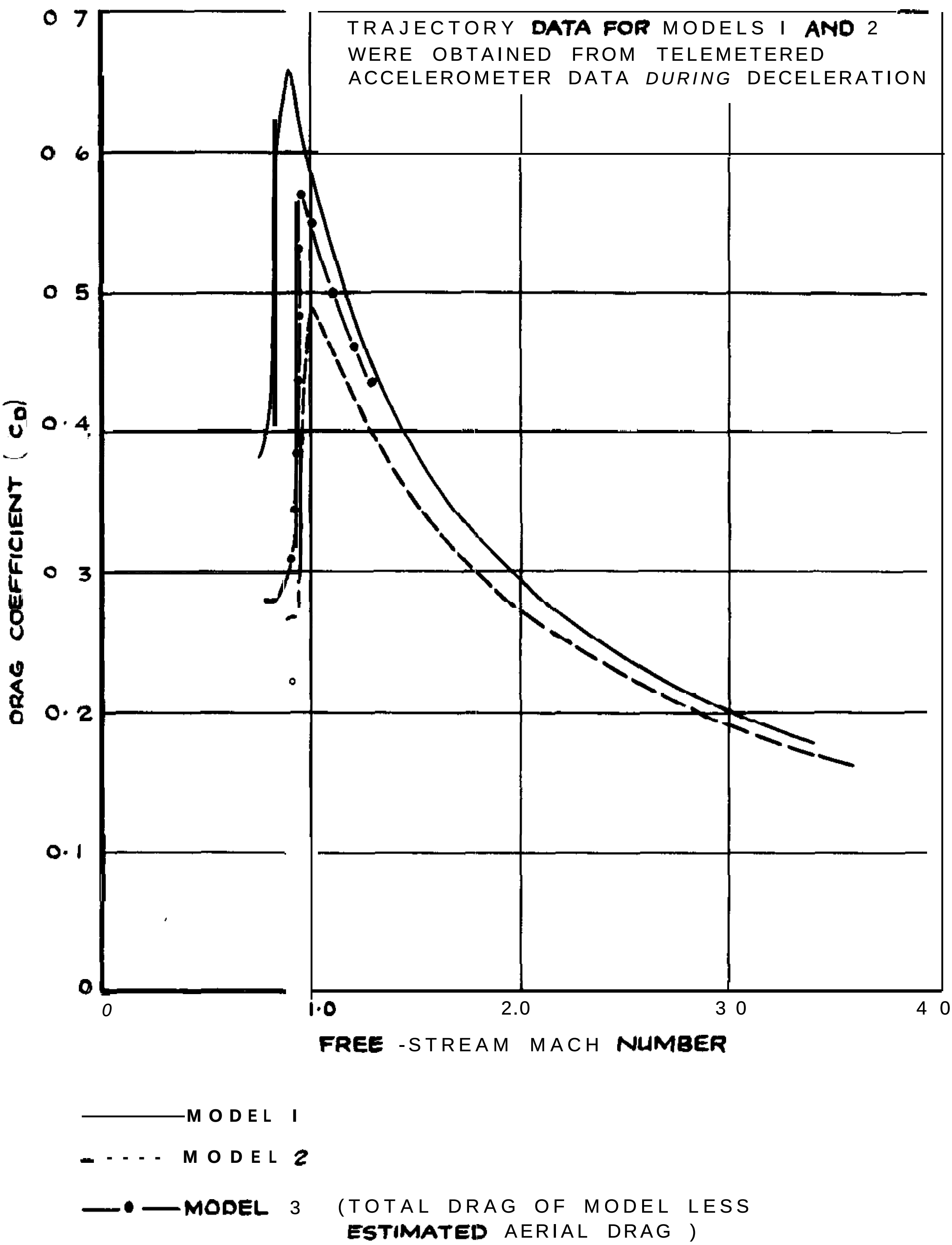

FIG. 9 COMPARISON OF TOTAL DRAGS OF CONES

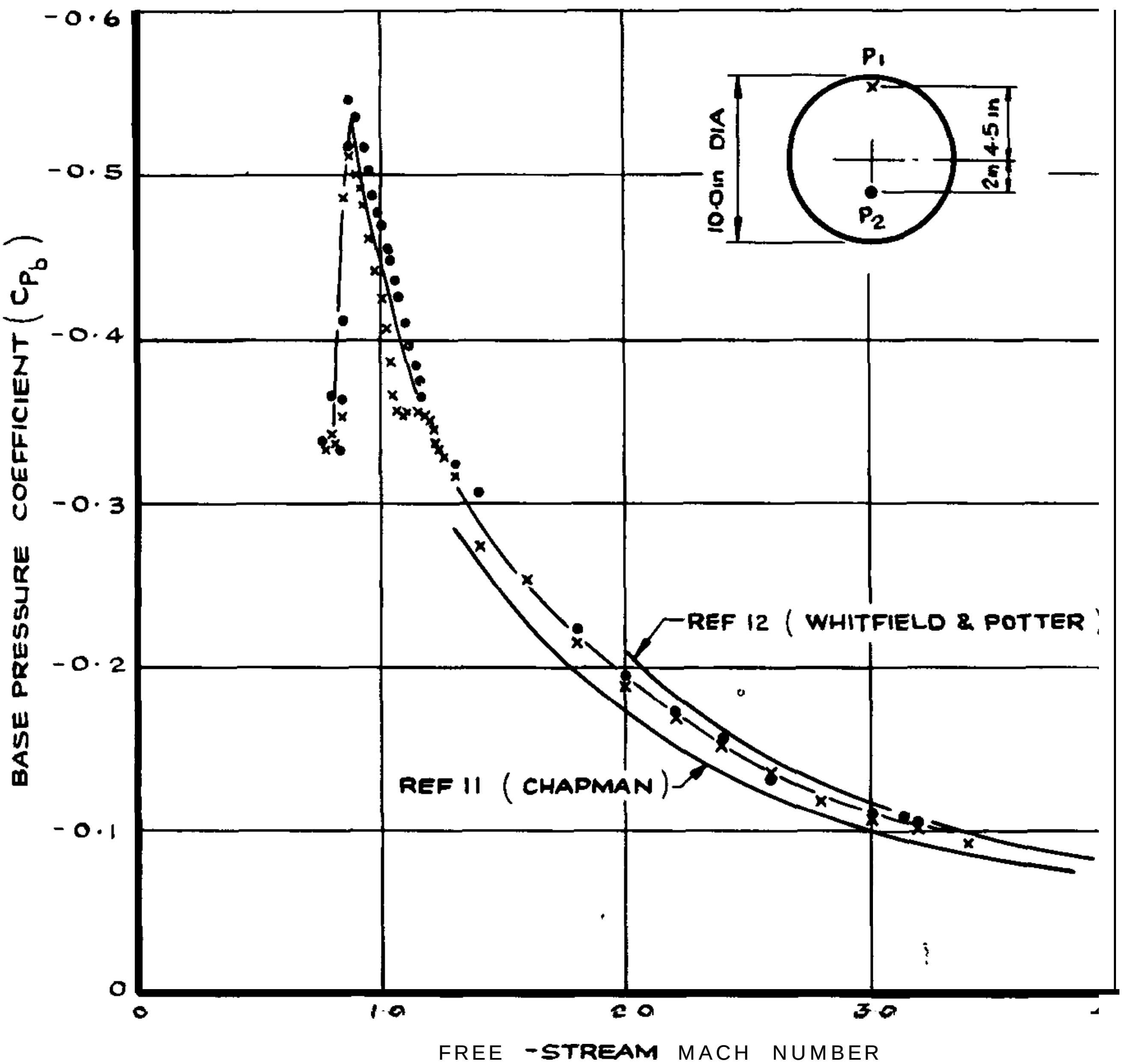

FIG. 10a VARIATION OF BASE PRESSURE WITH MACH NUMBER FOR MODEL I

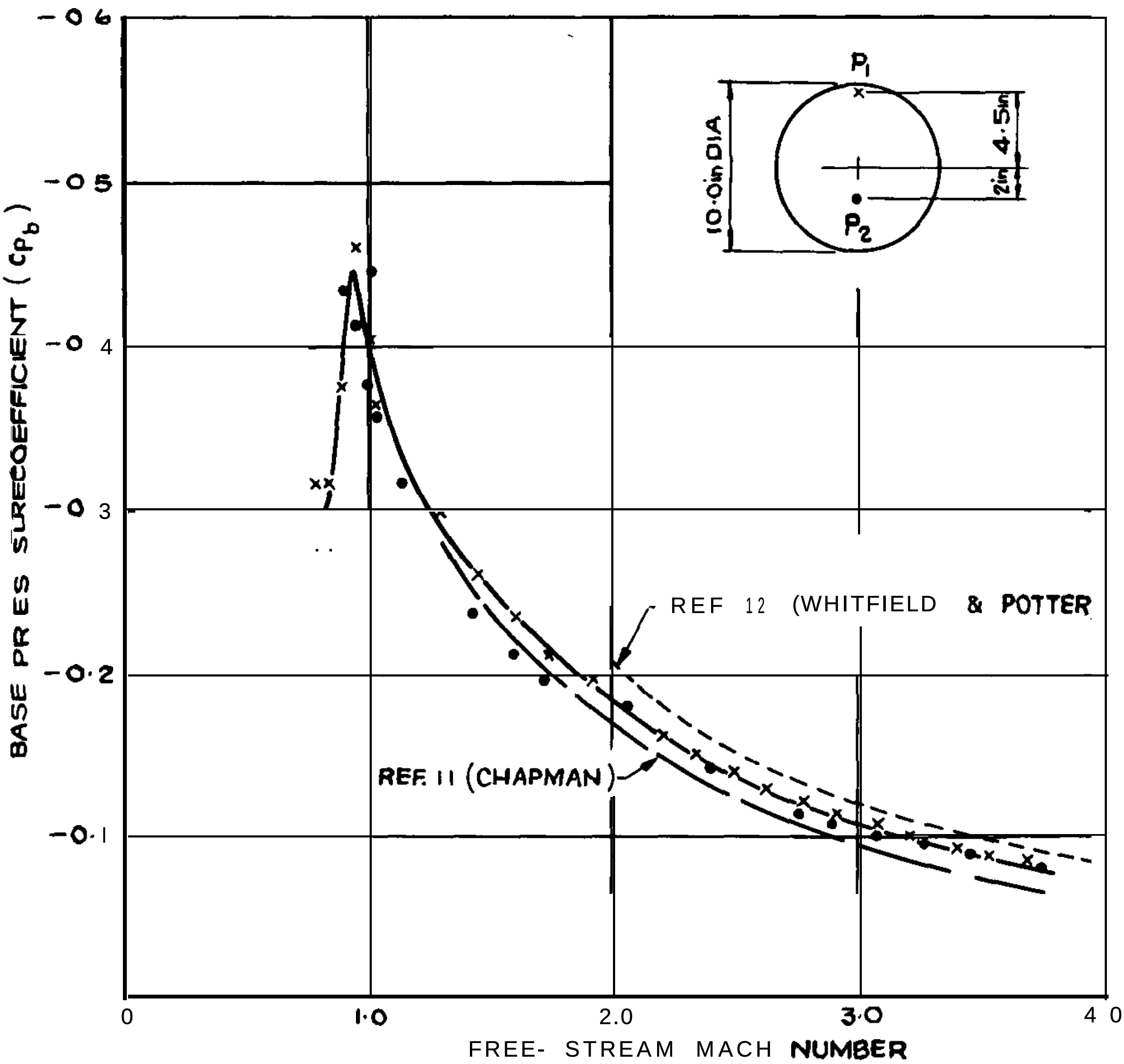

(MACH NUMBER DERIVED USING METHOD B OF SECTION 5.1)

FIG. 10b VARIATION OF BASE PRESSURE WITH MACH NUMBER FOR MODEL 2

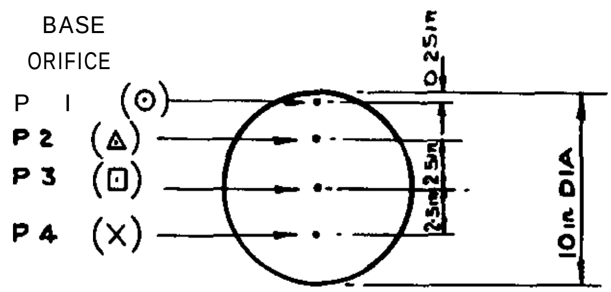

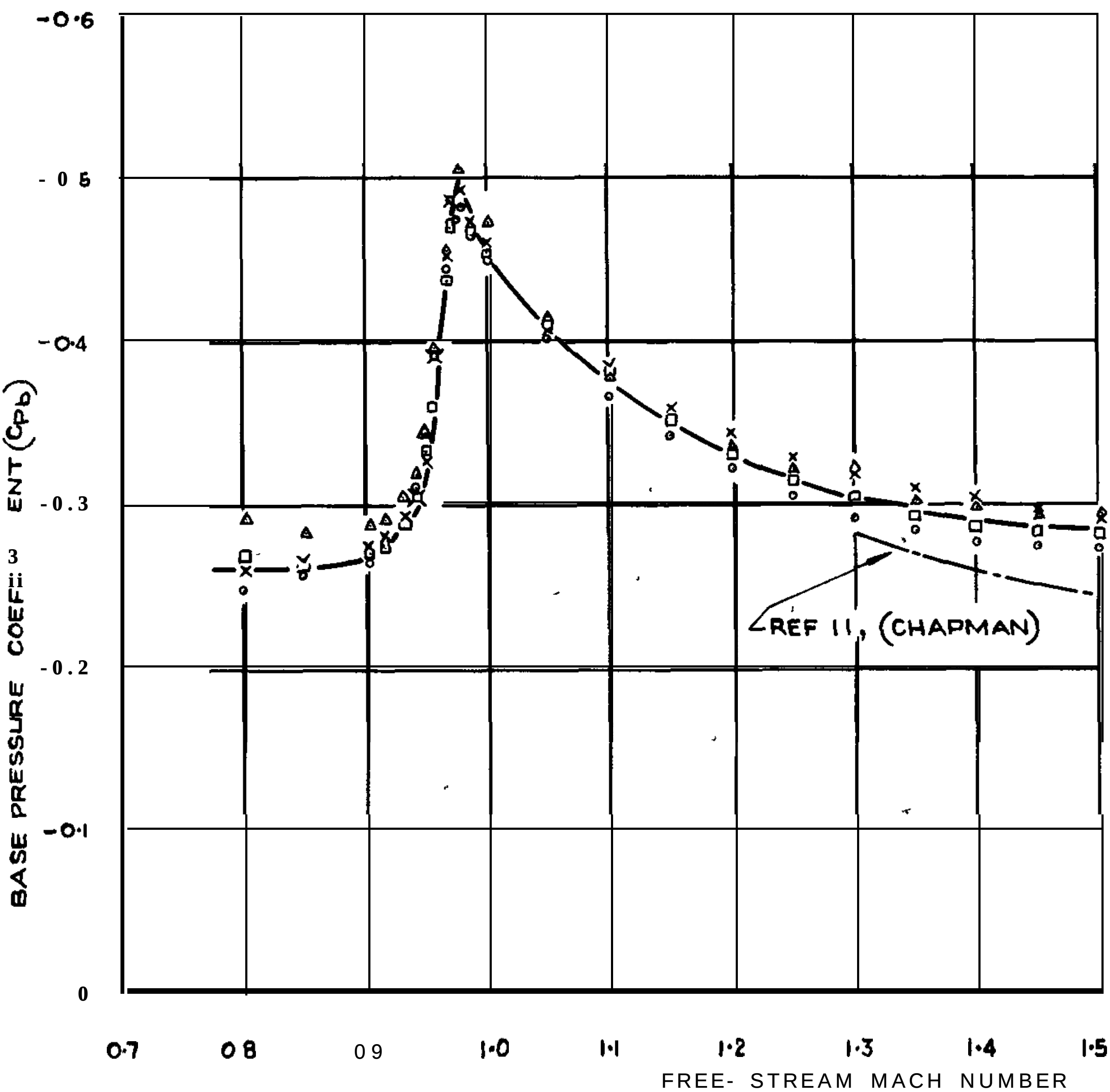

FIG. 10c VARIATION OF BASE PRESSURE WITH MACH NUMBER FOR MODEL 3

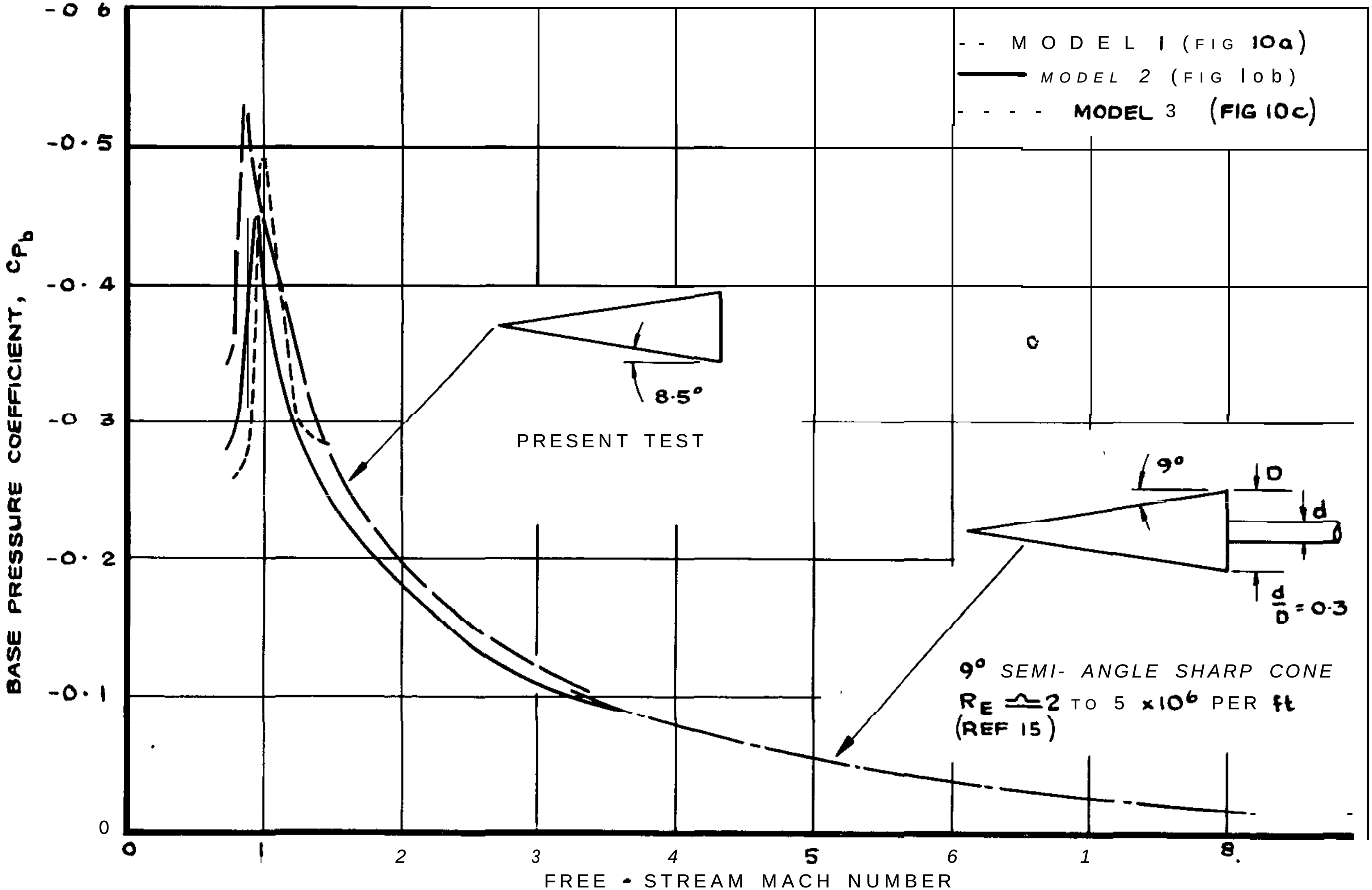

FIG. 11a COMPARISON OF BASE PRESSURE COEFFICIENTS

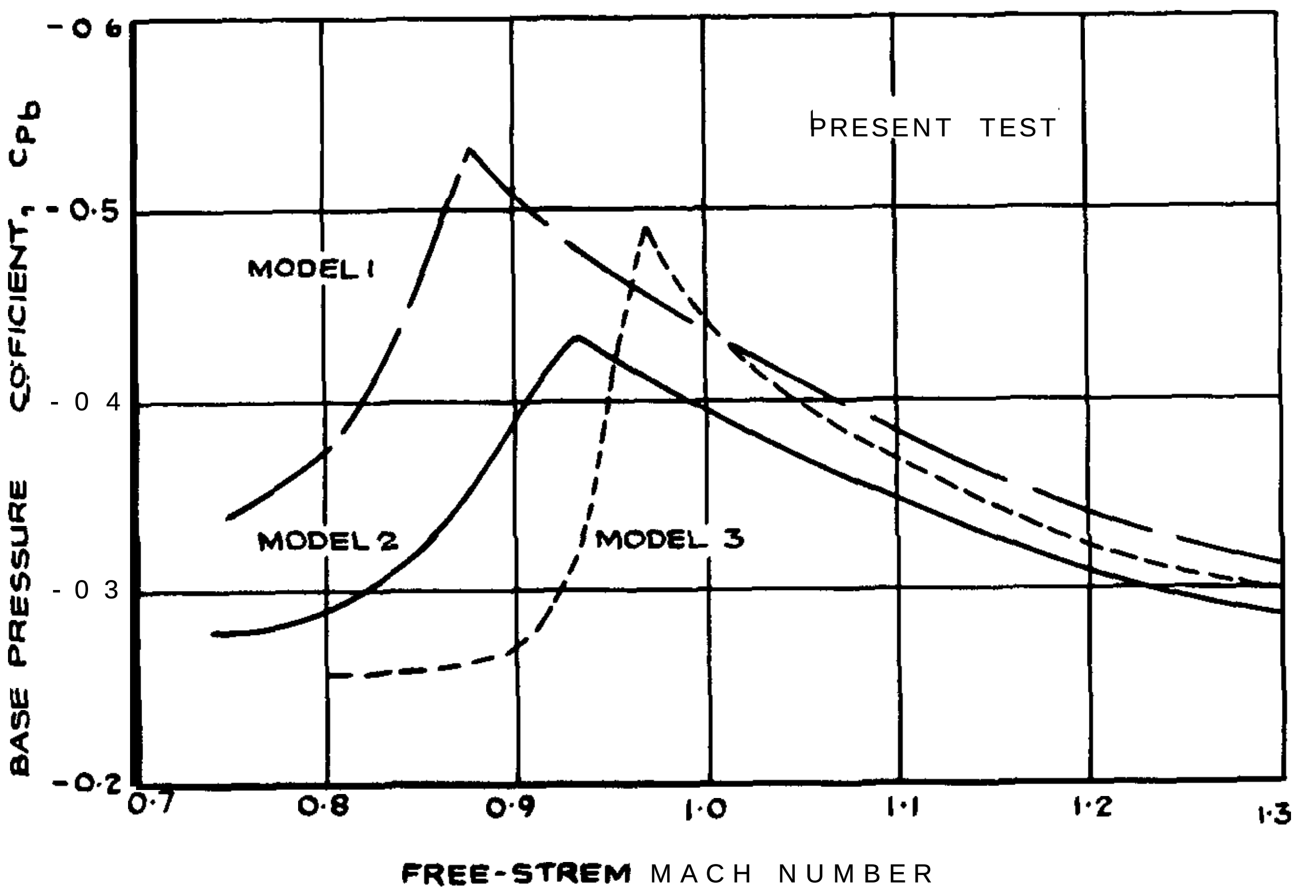

FIG. I lb COMPARISON OF BASE PRESSURE COEFFICIENTS

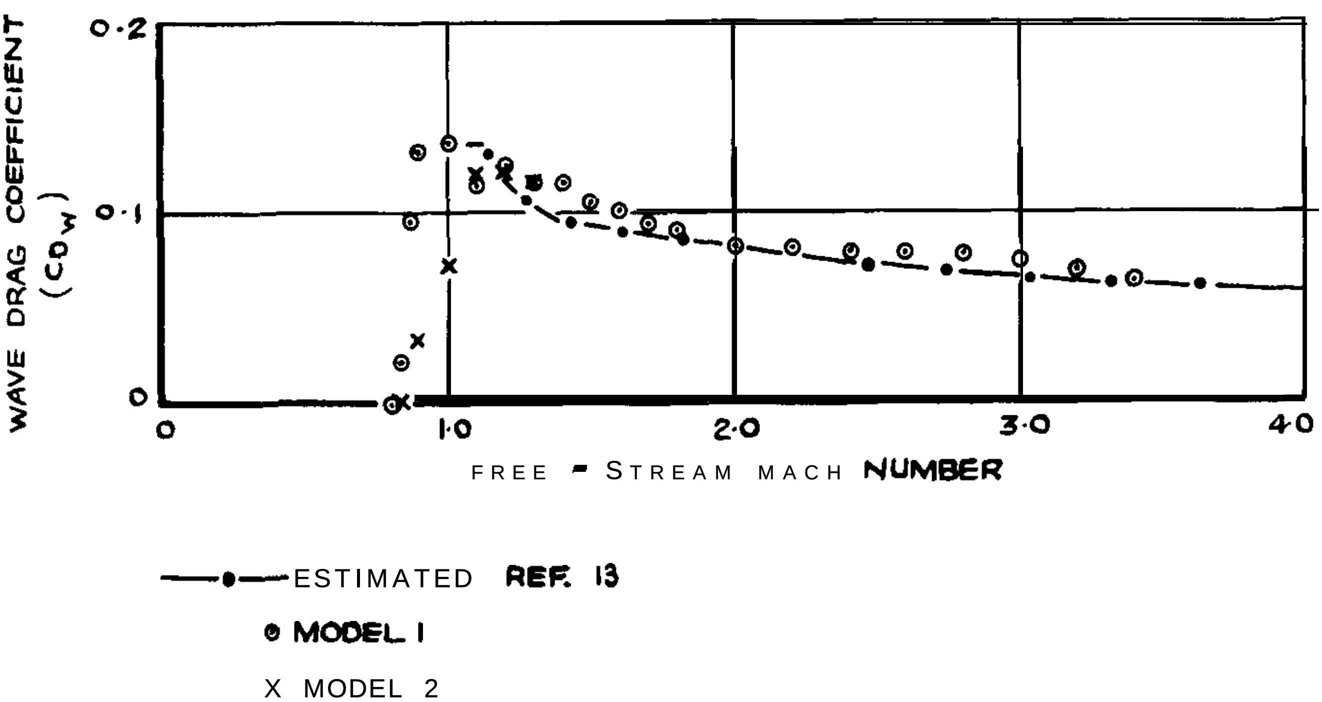

C_{D_W} (MODEL 1) = $C_{D\ TOTAL} - [C_{D_{BASE}} + C_{D_{SKIN}}]$ FROM FIG 8a

C_{D_W} (MODEL 3) = $C_{D\ TOTAL} - [C_{D_{BASE}} + \overline{C_{D_{SKIN}}} + C_{D_{AERIALS}}]$ FROM FIG 8b

FIG. 12 COMPARISON OF EXPERIMENTAL WAVE DRAG WITH THEORY

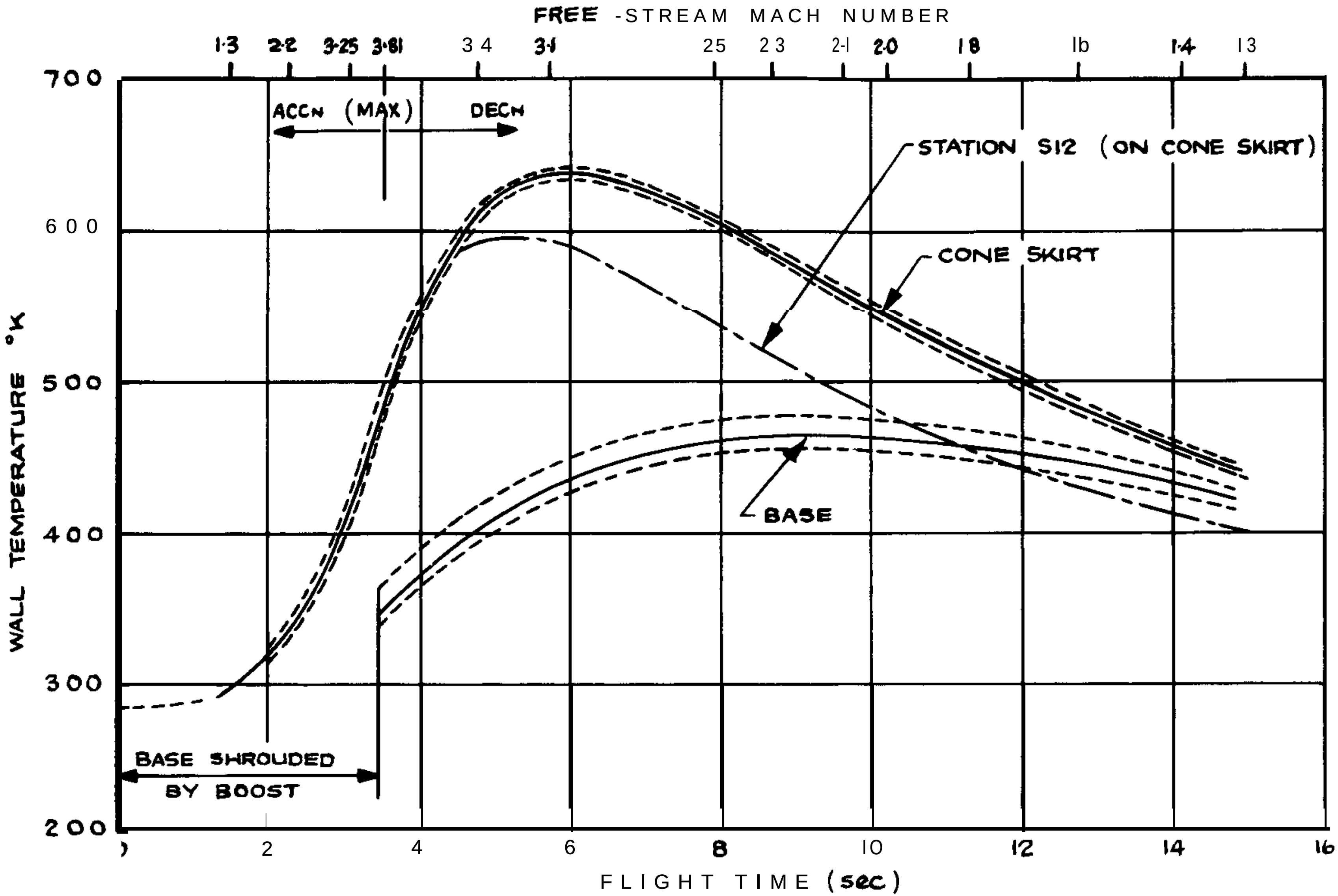

----- — — — LIMITS OF INDIVIDUAL STATION MEASUREMENTS

FIG. 13 WALL TEMPERATURE HISTORIES FOR MODEL 2

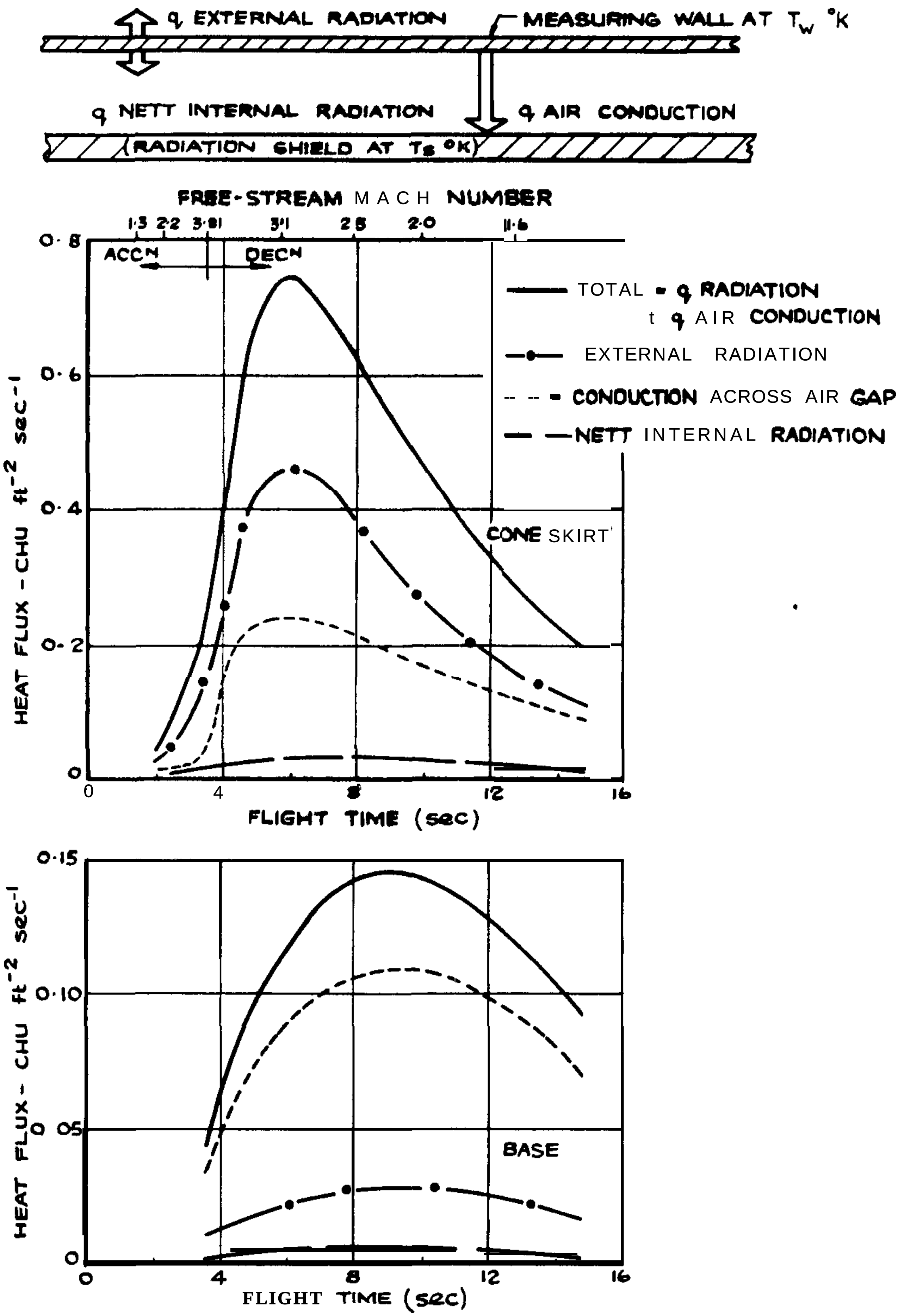

FIG.14 CORRECTIONS TO EXPERIMENTAL HEAT FLUX FOR RADIATION AND INTERNAL CONDUCTION

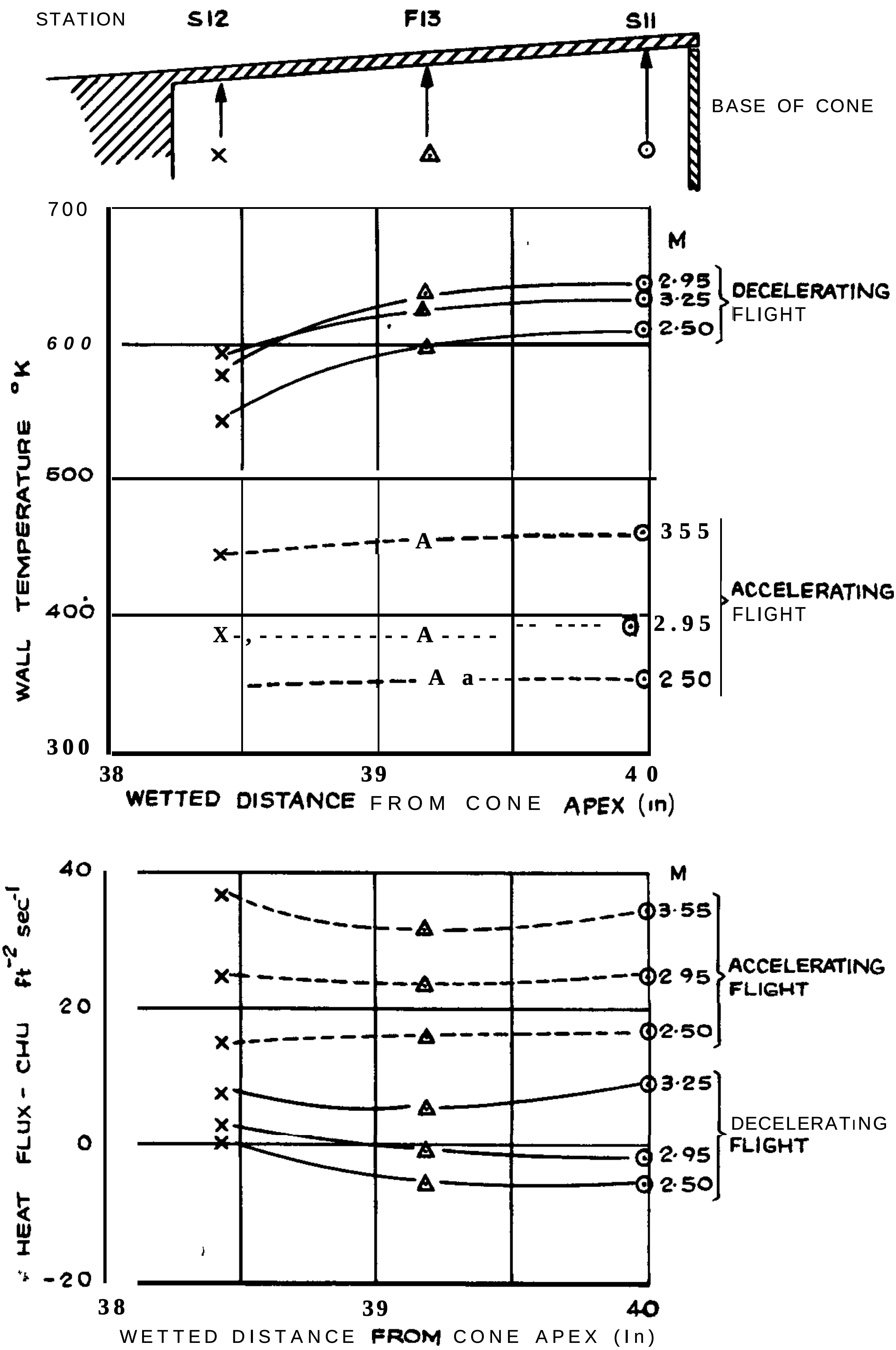

FIG. 15a TEMPERATURE AND HEAT FLUX DISTRIBUTIONS ALONG CONE SKIRT

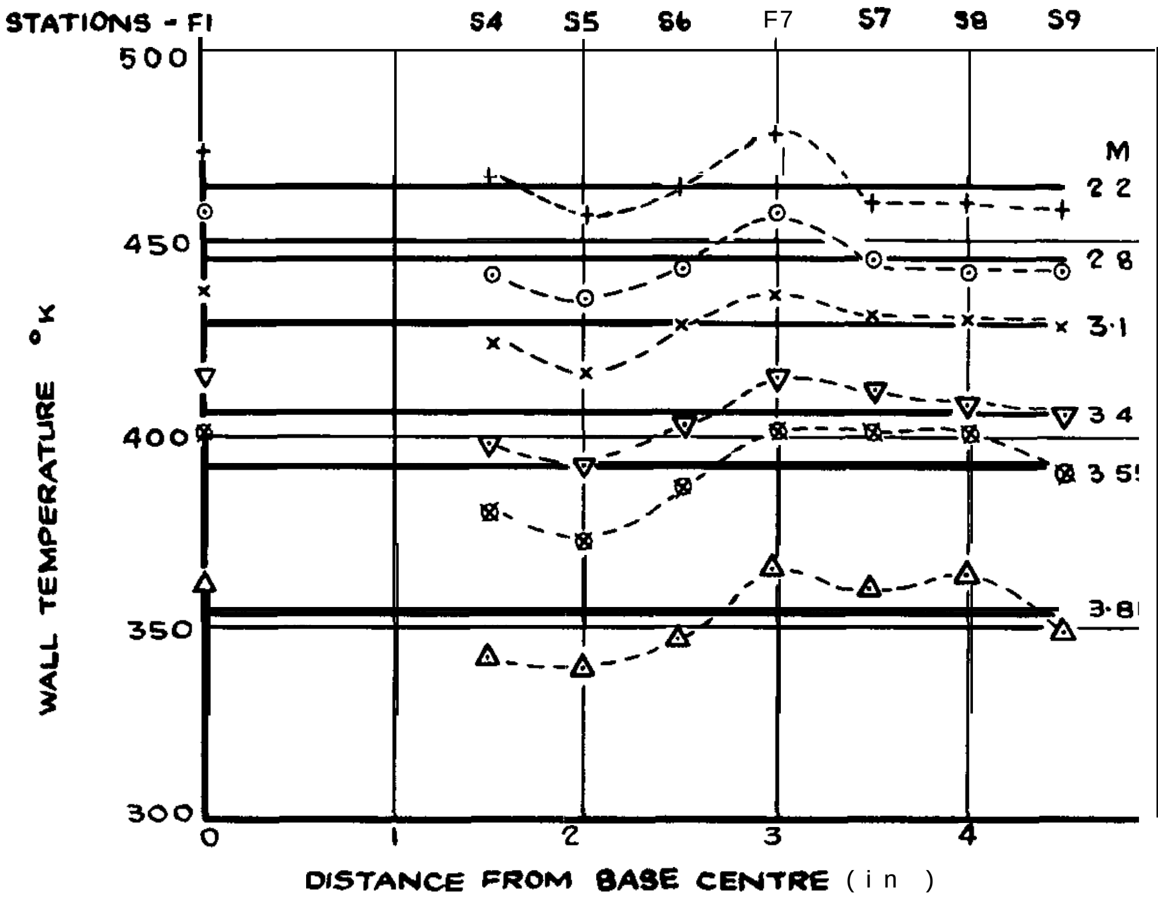

TEMPERTURE OF BASE

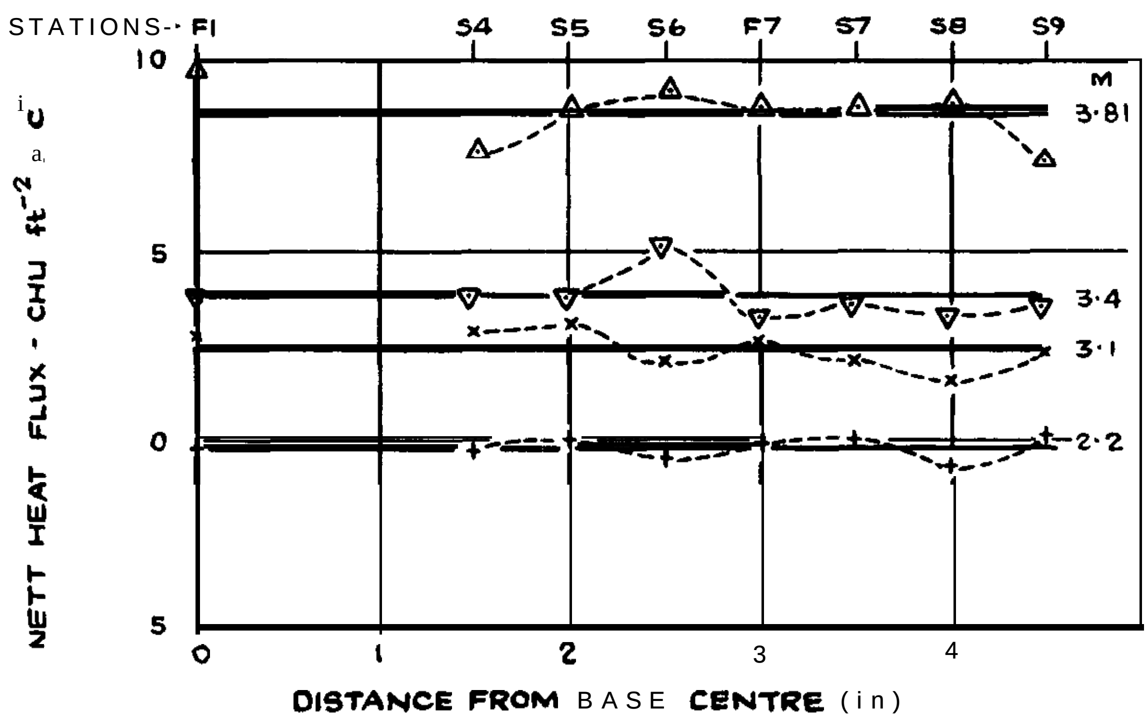

HEAT FLUX TO BASE

FIG 15b TEMPERATURE 8 HEAT FLUX DISTRIBUTIONS AT VARIOUS MACH NUMBERS OVER BASE

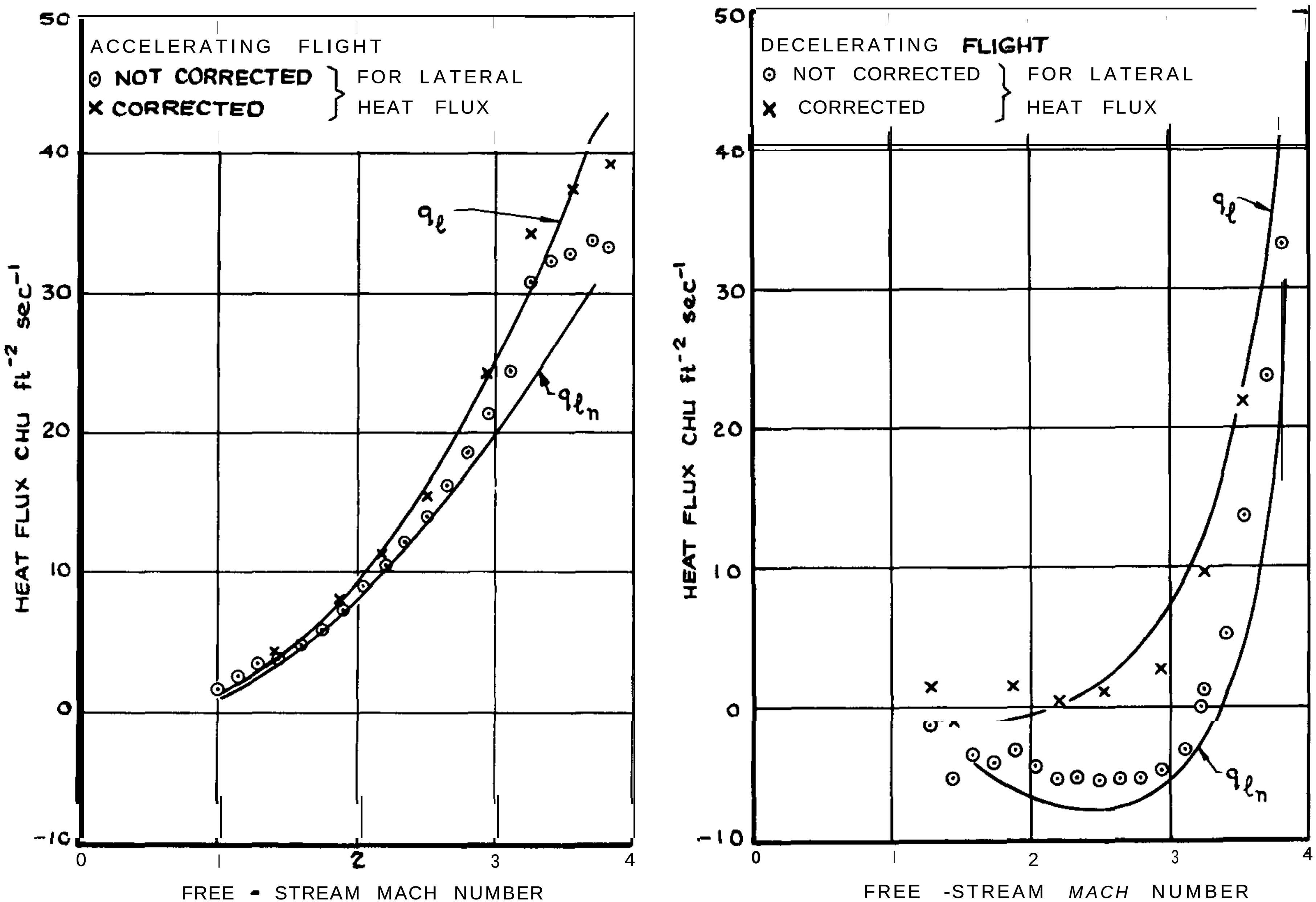

STATION S 12

FIG. 16a VARIATION OF HEAT FLUX WITH MACH NUMBER OVER CONE SKIRT

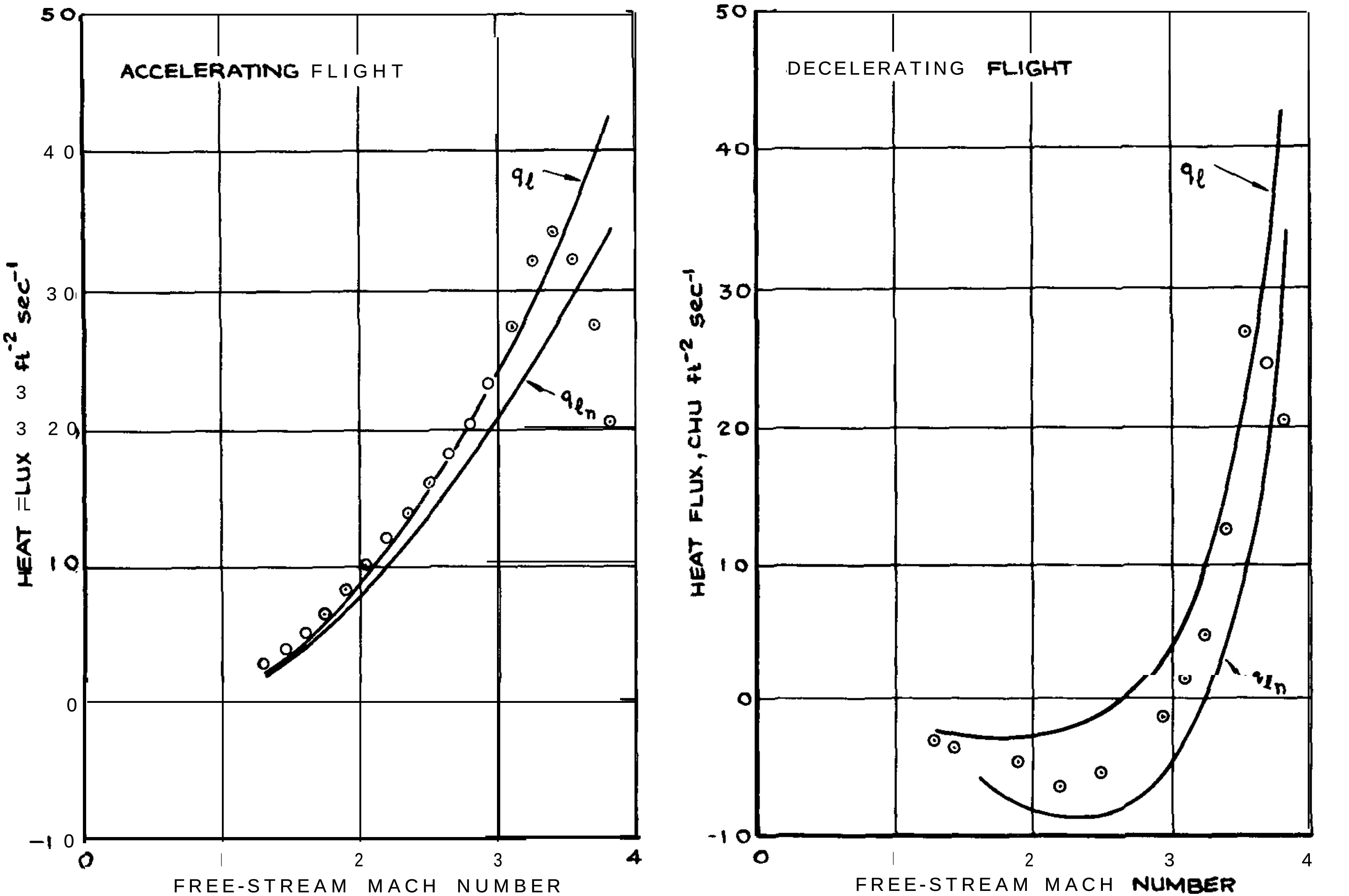

STATION F13

FIG. 16a cont VARIATION OF HEAT FLUX WITH MACH NUMBER OVER CONE SKIRT

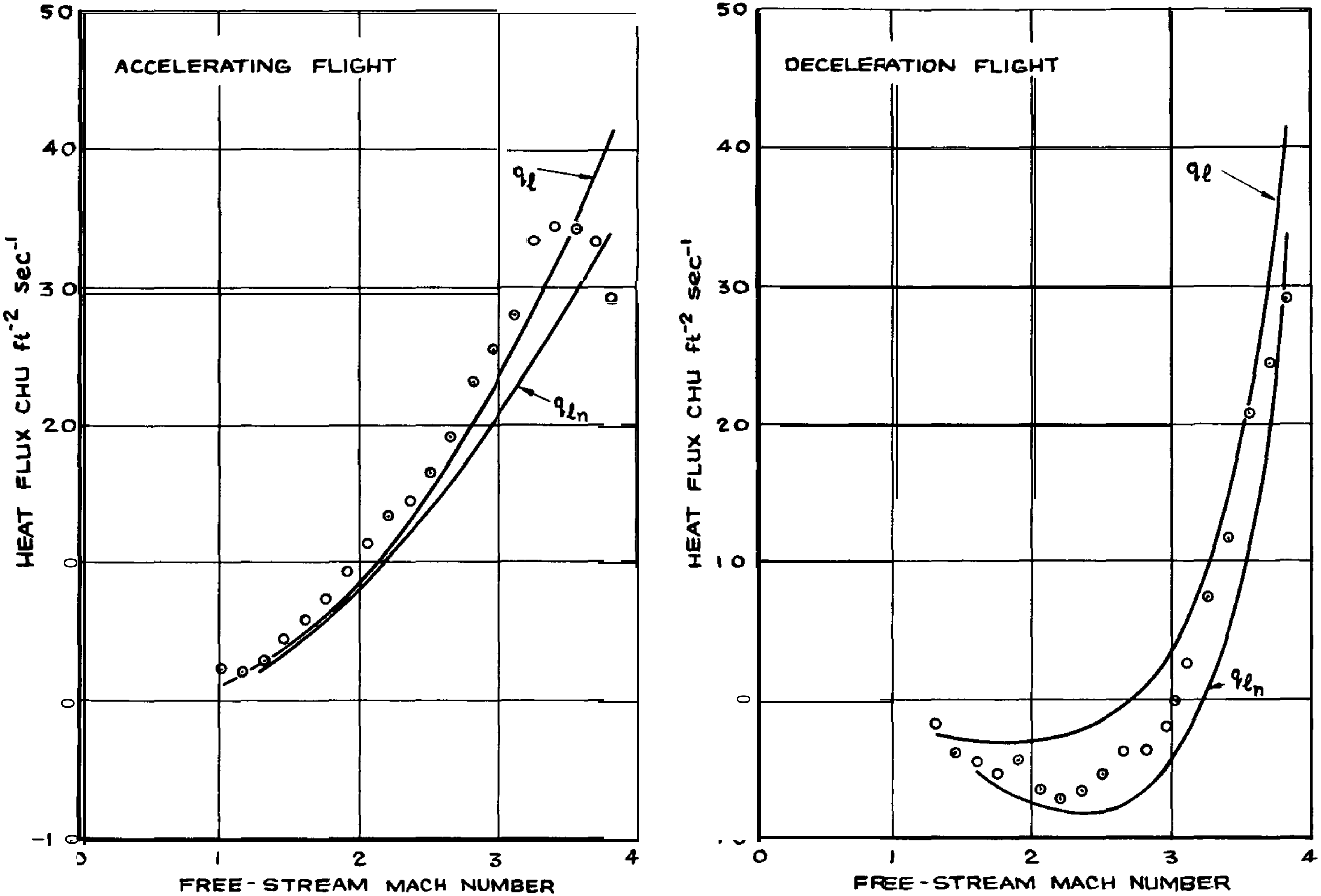

STATION S11

FIG. 16a concld VARIATION OF HEAT FLUX WITH MACH NUMBER OVER CONE SKIRT

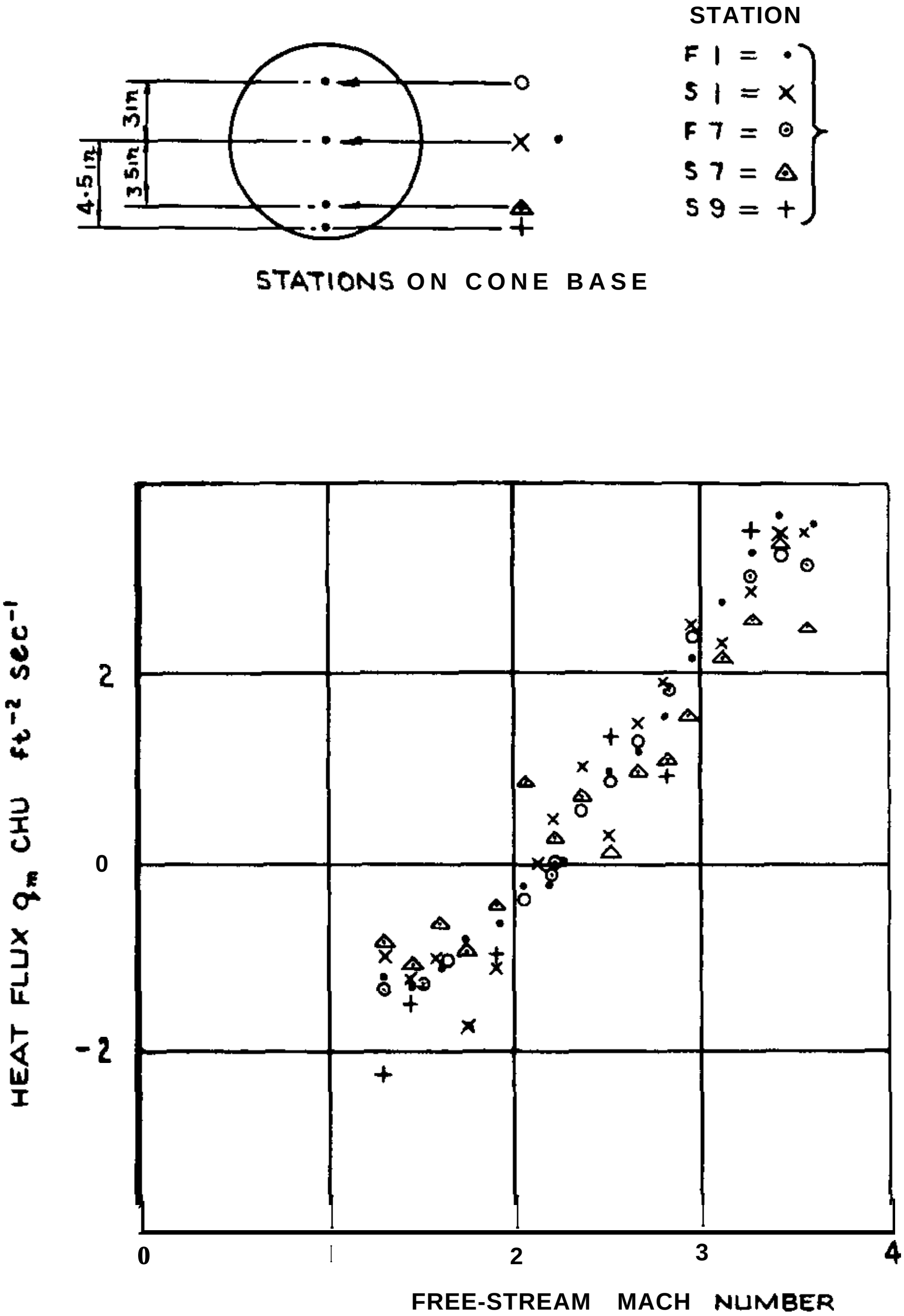

FIG. 16 b TYPICAL VARIATION OF HEAT FLUX WITH MACH NUMBER OVER CONE BASE .(DECELERATING FLIGHT)

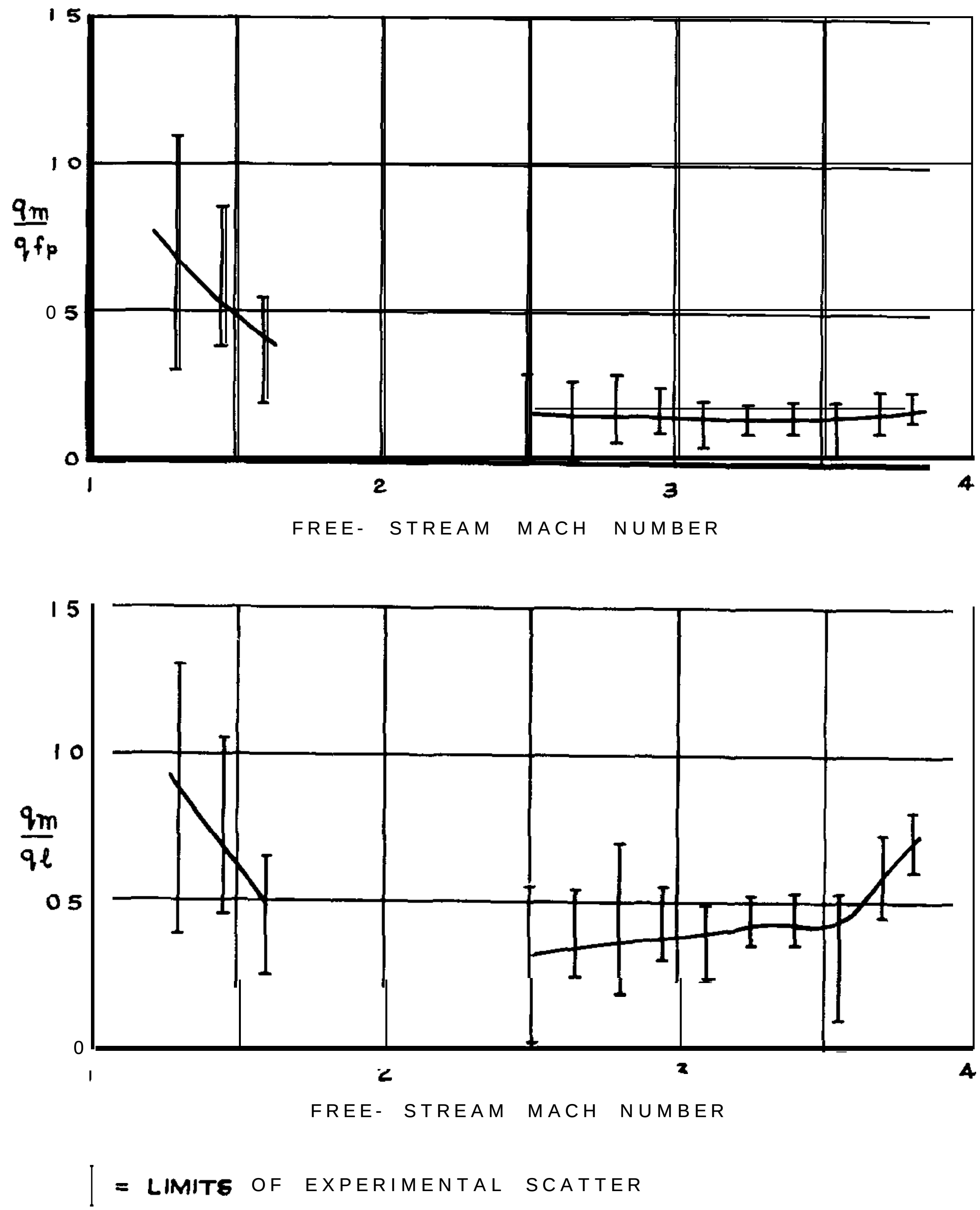

FIG. 17 COMPARISON OF MEASURED 8 REFERENCE HEAT FLUXES T o BASE (DECELERATING FLIGHT)

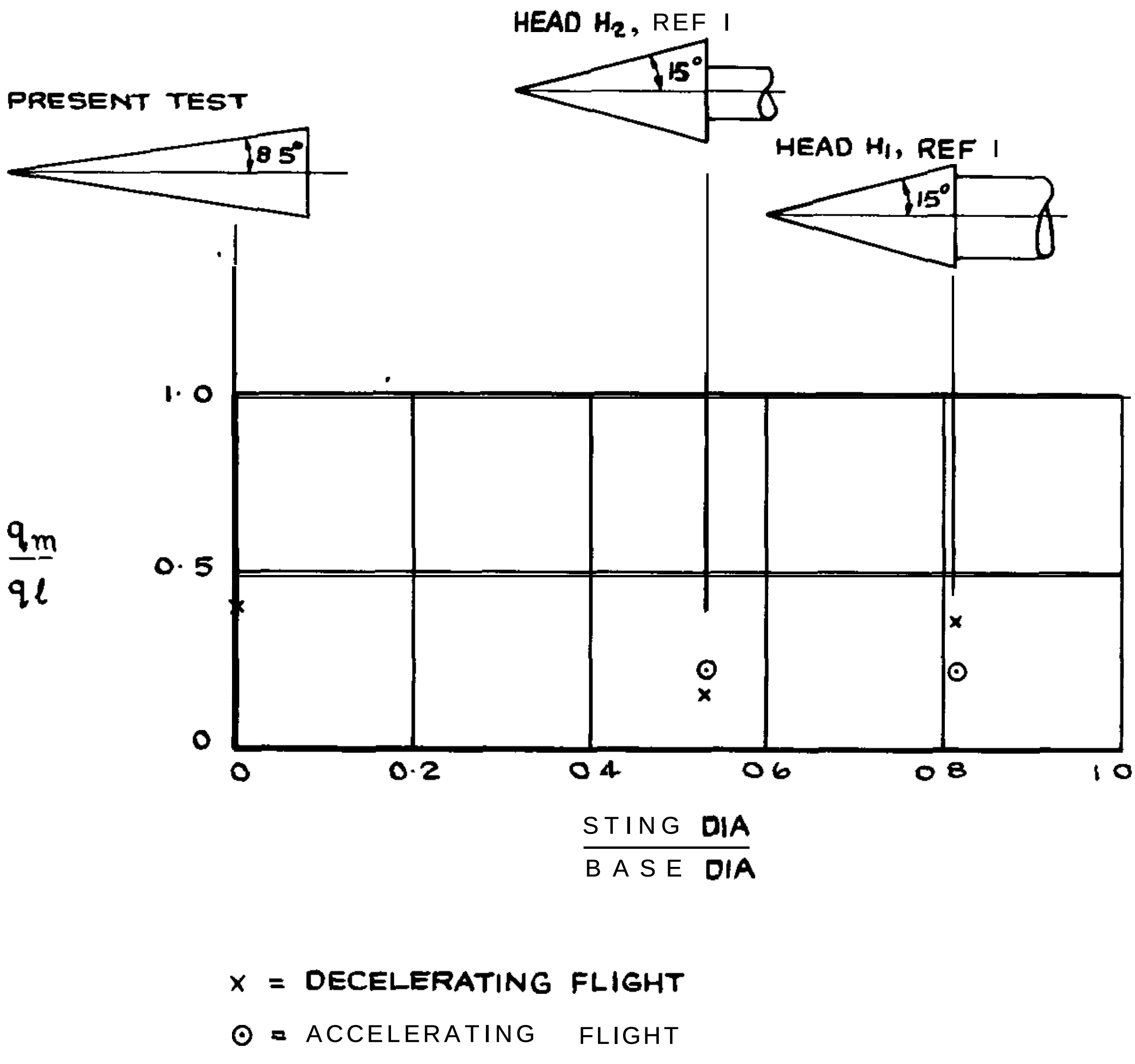

FIG 18 EFFECT OF STING ON HEAT TRANSFER TO BASE $(M = 3 \cdot 5)$

Printed in England for Her Majesty's Stationery Office
the Royal Aircraft Establishment, Farnborough. Dd.129528 K4

A.R.C. C.P. 958
December 1966
Greenwood, G.H.

533.696.24 :
533.6.048.2 :
533.6.011.6

MEASUREMENTS OF DRAG. BASE PRESSURE AND BASE AERODYNAMIC HEAT TRANSFER APPROPRIATE TO 8.5° SEMI-ANGLE SHARP CONES IN FREE FLIGHT AT MACH NUMBERS FROM 0.8 TO 3.8

Measurements or drag, base pressure and aerodynamic heat transfer have been made on a sharp cone in free flight at Mach numbers up to 3.8 and free stream Reynolds numbers Up to 77 millions based on cone length. The drag and base pressure measurements were in good agreement with estimates. The heat transfer data were however degraded by deficiencies in the construction of the thermocouples. Nevertheless they did show that the aerodynamic heat flux was uniform over the base. I” particular there was no evidence of high values at the rear stagnation point.

A.R.C. C.P. 958
December 19%
Greenwood, G.H.

533.696.24 :
533.6.048.2 :
533.6.011.6

MEASUREMENTS OF DRAG, BABE PRESSURE AND BASS AERODYNAMIC HEAT TRANSFER APPROPRIATE TO 8.5° SEMI-ANGLE SHARP CONES IN FREE FLIGHT AT MACH NUMBERS FROM 0.8 TO 3.8

Measurements of drag, base pressure and aerodynamic heat transfer have been made on a sharp cone 1” free flight at Mach numbers up to 3.8 and free stream Reynolds ““tiers up to 77 millions based 0” cone length. The drag and base pressure measurements were in good agreement with estimates. The heat transfer data were however degraded by deficiencies in the construction or the thermocouples. Nevertheless they did show tit the aerodynamic heat flux was uniform over the base. In particular there was no evidence of high values at the rear stagnation point.

A.R.C. C.P. 958
December 1966
Greenwood, O.H.

533.696.24 :
533.6.048.2 :
533.6.011.6

MEASUREMENTS OF DRAG, BABE PRESSURE AND BASE AERODYNAMIC HEAT TRANSFER APPROPRIATE TO 8.5° SEMI-ANGLE SHARP CONES IN FREE FLIGHT AT MACH NUMBERS FROM 0.8 TO 3.8

Measurements of drag, base pressure and aerodynamic heat transfer have been made on a sharp cone in free flight at Mach numbers up to 3.8 and free stream Reynolds numbers up to 77 millions based on cone length. The drag and base pressure measurements were in good agreement with estimates. The heat transfer data were however degraded by deficiencies in the construction of the thermocouples. Nevertheless they did show that the aerodynamic heat flux was uniform over the base. In particular there was no evidence of high values at the rear stagnation point.

DETACHABLE ABSTRACT CARDS

C.P. No. 958

Published by
HER MAJESTY'S STATIONERY OFFICE

To be purchased from
49 High Holborn, London W C I
423 Oxford Street. London W 1
13.4 Castle Street, Edinburgh 2
109 St Mary Street, Cardiff
Brazennose Street. Manchester 2
50 Fairfax Street, Bristol 1
35 Smallbrook, Ringway. Birmingham 5
7-11 Linenhall Street, Belfast 2
or through any bookseller

C.P. No. 958

S.O. CODE No. 23-9017-58